Shobiha K. Premkumar

Subject Identification using EEG Signals and Supervised Learning

Master's thesis in Cybernetics and Robotics

Supervisor: Marta Molinas

June 2020

Master's thesis

NTNU
Norwegian University of Science and Technology
Faculty of Information Technology and Electrical Engineering
Department of Engineering Cybernetics

NTNU
Norwegian University of
Science and Technology

Shobiha K. Premkumar

Subject Identification using EEG Signals and Supervised Learning

Master's thesis in Cybernetics and Robotics
Supervisor: Marta Molinas
June 2020

Norwegian University of Science and Technology
Faculty of Information Technology and Electrical Engineering
Department of Engineering Cybernetics

NTNU

Kunnskap for en bedre verden

Abstract

This thesis investigates the use of electrical brain signals captured in Electroencephalography (EEG) as a parameter for a biometric system. The captured brain signals are utilized to create a Subject Identification system for real-time classification. The system was designed by analyzing two types of classification techniques offline: Machine Learning (ML) and Deep Learning (DL). To reduce the computational complexity in real-time classification, channel reduction, and dimension reduction was also studied. The methods were examined on two different neuro-paradigms: resting-state and event-related potential (ERP).

In order to use ML as a classification technique, the EEG signals were first decomposed to obtain meaningful physical signals using Empirical Mode Decomposition (EMD), Discrete Wavelet Transform (DWT), and frequency bands. Various features (energy, fractal, statistical, and HHT-based) were then extracted from the signals and used as input on five different ML algorithms to create classification models. The models were utilized to identify unique patterns in EEG-signals to identify subjects. Principle Component Analysis (PCA) was used as a method for dimension reduction. The Principle Components (PCs) found using PCA were also used as input to the ML algorithms. Before any classification, the EEG-signals were pre-processed to improve the Signal-to-Noise ratio (SNR).

The highest accuracy of 1.00 was obtained using ML as a classification technique with DWT using mother wavelet Symlet 7 (Sym7) as a basis to extract energy features and the k-Nearest Neighbors (k-NN) classification algorithm on pre-processed EEG-signals without channel reduction. The second classification technique used raw EEG-signals as input to a Convolutional Neural Network (CNN), resulting in its highest accuracy of 0.95 when using EEG-signals without channel reduction. Both classification techniques used resting-state as neuro-paradigm when achieving their highest accuracy.

A simulated EEG-based Subject Identification system was then created based on results from offline-classification. The system was created using DWT with mother wavelet Sym7 to extract statistical features and Naive Bayes (NB) as the classification algorithm. The system was tested on pre-processed EEG-data containing five channels from the resting-state neuro-paradigm. A True Acceptance Rate (TAR) of 0.93 was achieved using 40 subjects. The obtained results show that the use of DWT and statistical features with the NB classifier is suitable for developing an EEG-based Subject Identification system when using resting-state as neuro-paradigm. This also encourages further research on utilizing electrical brain signals as a biometric.

Abstrakt - Norwegian

Denne masteroppgaven undersøker bruken av elektriske hjernesignaler fanget i elektroencefalografi (EEG) som parameter for et biometrisk system. De fangede hjernesignalene brukes til å lage et person-identifikasjonssystem for sanntids klassifisering. Systemet ble designet ved å analysere to typer klassifiseringsteknikker offline: maskinlæring (ML) og dyp læring (DL). For å redusere beregningskompleksiteten i sanntids klassifisering, ble kanalreduksjon og dimensjonsreduksjon også studert. Metodene ble undersøkt på to forskjellige neuro-paradigmer: hviletilstand og hendelsesrelatert potensial (ERP).

For å bruke ML som klassifiseringsteknikk ble EEG-signalene først dekomponert for å oppnå meningsfulle fysiske signaler ved bruk av *Empirical Mode Decomposition* (EMD), *Discrete Wavelet Transform* (DWT) og frekvensbånd. Ulike egenskaper (energi, fraktal, statistisk og HHT-basert) ble deretter trukket ut fra signalene og brukt som inndata på fem forskjellige ML-algoritmer for å lage klassifiseringsmodeller. Modellene ble brukt til å identifisere unike mønstre i EEG-signaler for å identifisere personer. Prinsipal komponent analyse (PCA) ble brukt som metode for dimensjonsreduksjon. Prinsipal komponentene (PC) som ble funnet ved bruk av PCA, ble også brukt som inndata til ML-algoritmene. Før klassifisering ble EEG-signalene forbehandlet for å forbedre signal-til-støy-forholdet (SNR).

Den høyeste nøyaktighet på 1.00 ble oppnådd ved bruk av ML som klassifiseringsteknikk med DWT ved bruk av mor-wavelet *Symlet 7* (Sym7) som grunnlag for å trekke ut energiegenskaper og k-nærmeste naboer (k-NN) som klassifiseringsalgoritme på forbehandlet EEG-signaler uten kanalreduksjon. Den andre klassifiseringsteknikken brukte rå EEG-signaler som inndata til et *Convolutional Neural Network* (CNN), som resulterte i den høyeste nøyaktighet på 0.95 ved bruk av EEG-opptak uten kanalreduksjon. Begge klassifiseringsteknikkene brukte hviletilstand som nevroparadigme når de oppnådde sin høyeste nøyaktighet.

Et simulert EEG-basert person-identifikasjonssystem ble deretter opprettet basert på resultater fra offline-klassifisering. Systemet ble opprettet ved å bruke DWT med mor-wavelet Sym7 for å trekke ut statistiske egenskaper og Naive Bayes (NB) som klassifiseringsalgoritme. Systemet ble testet på forbehandlet EEG-data som inneholdt fem kanaler fra hviletilstandens neuro-paradigmen. En *True Acceptance Rate* (TAR) på 0.93 ble oppnådd ved bruk av 40 forsøkspersoner. De oppnådde resultatene viser at bruk av DWT og statistiske funksjoner med NB-klassifiseringen er egnet for å utvikle et EEG-basert person-identifikasjonssystem når man bruker hviletilstand som nevroparadigme. Dette oppmuntrer også til videre forskning på bruk av elektriske hjernesignaler som biometri.

Acknowledgment

Firstly, I want to thank my supervisor Marta Molinas for giving me a chance to work with this project and introducing me to this field of research. I would especially like to thank co-supervisor Luis Alfredo Moctezuma, for giving guidance and valuable feedback on my specialization project and master thesis.

My acknowledgment also goes to NTNU's IDUN support for guidance on how to use the school servers for training classification models and the community at Stack Overflow for technical support.

I want to thank my friends and family for help and support along the way. Thank you to Sarah Sayeed Qureshi, Atussa Koushan, Tonja Joseph and Mia Pin Berge for listening and mental motivation through all of my master's degree.

Finally, my special thanks go to my father for giving me his time for discussion and interest in my master's project.

Shobiha K. Premkumar

Preface

This master thesis is the last part of a Master of Technology in Cybernetics and Robotics. The master thesis was written during the spring semester of 2020 with the Department of Engineering Cybernetics at the Norwegian University of Science and Technology (NTNU), supervised by Professor M. Molinas.

The datasets used in this work were provided by L. A. Moctezuma and collected by the Network-BMI Brain Database Project (NBP). The NBP Data are provided by Advanced Telecommunication Research Institute International, Kyoto, Japan. The REST API and database created for the real-time system is based on work by L.A. Moctezuma and M. Moussabbih. The feature extraction part in section 4.6.1 is based on work by L.A. Moctezuma. The Army Research Laboratory developed the deep learning architecture utilized in section 4.6.2. Computations in this work were performed on resources provided by the NTNU IDUN/EPIC computing cluster.

Portions of Ch. 1-2 are presented in my semester project "EEG-based Biometric System for Subject Identification using Empirical Mode Decomposition and Frequency Bands" (NTNU, 2019). These topics are presented in my master thesis to perceive the full picture of the work. The state-of-the-art literature presented in Ch. 3 is introduced by L.A. Moctezuma and myself, formulated by me. The results and analysis presented in Ch. 6 and conclusion in Ch. 7 are my original work.

The occurrence of COVID-19 has given some challenges while working on this thesis. There have been challenges with the task description that had to be adjusted along the way and the execution. I usually discuss with my fellow students when I face challenges as it inspires me to find solutions, but it has not been possible during this time.

When starting with this project, I had no prior experience with EEG signals, nor signal analysis, machine learning, and database design. I have gained a variety of knowledge the past year, and hopefully, this is reflected in my master thesis.

Lørenskog, May 28. 2020 Shobiha K. Premkumar

Contents

List of Tables

List of Figures

List of Acronyms

BCI Brain Computer Interface.

CAR Common Average Reference.

CNN Convolutional Neural Networks.

CWT Continuous Wavelet Transform.

DL Deep Learning.

DT Decision Tree.

DWT Discrete Wavelet Transform.

EEG Electroencephalography.

EEMD Ensemble Empirical Mode Decomposition.

EMD Empirical Mode Decomposition.

ERP Event Related Potential.

HFD Higuchi fractal dimension.

HHT Hilbert-Huang Transform.

HT Hilbert-Transform.

IMF Intrinsic Mode functions.

k-NN k-nearest neighbors.

LDA Linear Discriminant Analysis.

MI Mutual Information.

ML Machine Learning.

NB Naive-Bayes.

NN Neural Networks.

NSGA Non-dominated Sorting Genetic algorithm.

PC Principal Component.

PCA Principal Component Analysis.

PFD Petrosian fractal dimensions.

RF Random Forest.

SD Standard Deviation.

SVM Support Vector Machine.

VEP Visual Evoked Potential.

WT Wavelet Transform.

Chapter 1

Introduction

Since the early days' of communication, securing information has been an essential part of human existence. Early examples of securing data can be seen in Ancient Egypt who developed encryption using hieroglyphics, and Julius Caesar from Ancient Rome being the first person to use encryption for military purposes [1]. The shape of our modern world today has been formed by security. A prime example of this was breaking the German Enigma Machine, which was employed to encrypt the warfare data during the second world war. It was successfully decrypted by Alan Turning, striking as an example of creating and using secured information [2]. Security has again evolved into IT-security which comprises of technologies, processes, and controls designed to protect systems, networks, and data from attacks [3].

In civilian and government applications, establishing an individual's identity is of the highest importance, and errors in recognition can undermine the system's integrity. Some examples of such applications are access to bank safes, airport security, and international border control. Traditional methods for validating an individual's identity are using a combination of token-based methods (e.g., keys and ID-cards) and knowledge-based methods (e.g., passwords and PINs). However, traditional methods are vulnerable as they can be stolen by an imposter and not reliable when used in large-scale applications like border control [4]. In today's complex societies, accurate identification is becoming extremely important at the same rate as the problem of identifying a person is becoming more complicated, as the traditional methods are vulnerable for imposters and spoofing [5].

Biometrics is a method for identification based on a person's physiological (e.g., face, fingerprints) or behavioral characteristics (e.g., signature, voice). The traditional methods mentioned earlier utilizes "something that you possess "(e.g., ID-card) or "something that you remember "(e.g., password). The key to biometrics is that it represents a component of "something that you are," it cannot be misplaced or forgotten [5]. Conventional biometrics today, such as fingerprint, DNA, face, voice, and iris, has been widely adopted in real-life applications for identifica-

tion [6, 4]. Replacing traditional identification methods with biometrics is therefore introduced.

Biometrics may seem more secure than traditional tokens as they represent the user itself; however, biometrics do have their weaknesses. For instance, fingerprints can be faked through a variety of materials or by printing a 2D picture of the fingerprint, and DNA can be stolen from surfaces touched by the target subject [4]. Biometrics such as the face, fingerprints, and iris are noncancelable, meaning once stolen, they cannot be replaced - the user cannot change their face or grow a new finger. For a biometric to be more secure, it has to meet two criteria: be more difficult to steal and be cancelable. A biometric trait that fulfills these criteria are electric brain signals, which can be measured from the scalp using a technique known as EEG. [7].

Studies have shown that genetic and non-genetic factors can influence brain activity. It has also been demonstrated high individuality of EEG-signals among different people [8]. Thus, brain signals acquired using EEG have the potential to be used as a biometric, as the signals could be unique for each individual. Compared to other conventional biometrics, EEG has several unique advantages:

1. The user must be alive to produce EEG signals, as the lack of brain signals is an indication of brain death. Meanwhile, fingerprints, DNA, and face can be preserved even after people die [9].

2. The electrical brain activity is measured in voltage and needs to be measured with a short distance to the brain, making brain biometrics meet the criteria of being more challenging to steal.

3. EEG-signals are cancelable, as stolen or corrupted data can be replaced by new and different EEG-signals generated from another brain activity [7].

4. EEG can be used to detect and classify the level of stress, and associate it with the subject. This may protect the subject from being forced, as stress invalids the EEG-signals [7]. Additional layers for protection, such as detecting resting-state and the sex of the subject, can easily be added using EEG [10].

An EEG-based biometric system consists of two parts: the data acquisition part and the decision part. Data acquisition is the first part consisting of recording EEG-signals while the subject engages with a protocol, such as visual stimulation or resting-state. The second part is the decision part, where the acquired data is first pre-processed for increasing the Signal-to-Noise ratio (SNR) as EEG-signals recorded from the scalp are prone to noise. The next step consists of obtaining characteristic features of EEG signals with feature extraction. A model is then created using a classification technique and trained to classify the different sets of features. The trained model is then used to identify the subject by entering new EEG-signals.

The utilization of EEG as a biometric for identifying a subject is of interest. In the time being, adopting EEG in real-life applications is still not possible. There are seven factors in biometrics: universality, permanence, collectability, uniqueness, acceptability, acceptability, and circumvention [5, 4]. These factors are used to evaluate how reasonable a biometric is for use. Prior research has demonstrated universality, permanence, and uniqueness using brain biometrics. Despite the advantages of using EEG as a biometric compared to traditional biometrics, more research is necessary. Research is needed to improve the collectability, acceptability, and performance in EEG-based biometrics [11].

1.1 Problem description

This work investigates ML algorithms and DL as classification techniques for creating an EEG-based subject identification system. When testing ML as a technique for classification, signal analysis methods are applied for getting meaningful physical signals from EEG signals, and features are extracted from the signals for classification. A variety of features and classification algorithms are explored when using ML as a classification technique.

The task includes choosing a protocol by comparing previous research and by testing different neuro-paradigms on each classification technique. The classification accuracy when applying dimension reduction and reducing the number of EEG recordings channels is also investigated.

A simulated subject identification system with real-time classification is then implemented using one of the mentioned classification techniques. Real-time classification refers to the ability to give a rapid response when performing a classification to a user, which is required for any practical application.

The problem is approached by examining a variety of methods offline in search of the optimal method for real-time classification. The classification techniques are explored on two different datasets containing two types of neuro-paradigms: resting-state and cognitive task.

The simulated subject identification system for real-time classification is created as a part of a more extensive EEG-based biometric system containing an identification layer and authentification layer. This thesis focuses on the identification layer. The work on the authentication layer is presented in [12].

1.1.1 Limitations

Using a suitable dataset is essential for evaluating classification techniques. Due to COVID-19, it was not possible to create a dataset with a desired neuro-paradigm and test in a real scenario. Thus, already existing EEG datasets are utilized for analyzing different techniques in this work. This will affect the outcome from

different classification techniques as datasets used in this work are obtained from other experiments. When testing the application in real-time, the pre-existing datasets were used.

1.1.2 Research Questions

1. Can a generalized ML classification model be created for the same type of neuro-paradigm recorded from different protocols?

2. Is DL a suitable classification technique when using a reduced number of channels?

1.1.3 Motivation

Several organizations are using automated subject identification systems to improve customer satisfaction, secure critical resources, and enhance operating efficiency. Reliable biometric identification systems are used to serving these requests. Conventional biometrics are easy to use but cannot be reset once compromised. EEG signals can be reset like a password or an ID card, giving the possibility to be used as a biometric. This work motivates for designing reliable real-time EEG-based biometric systems for subject identification, and utilize electric brain signals as a secure biometric. EEG-based biometric systems hold the potential to be used in scenarios demanding high-security levels, such as financial agencies and defense systems.

1.2 Report structure

This report consists of seven chapters providing a comprehensive overview of knowledge to analyze electrical brain signals and design an EEG-based biometric system for subject identification. An overview of relevant background is presented in Ch.2. Related work in subject identification using EEG-signals is presented in Ch.3. Ch.4 outlines the methods used in offline classification. The implementation for real-time classification is described Ch.5. In Ch.6, the results obtained from offline and real-time classification, and the final system created, are presented and discussed. Ch.7, concludes and recommends future work for creating an EEG-based subject identification system.

Chapter 2

Background

This chapter provides relevant background knowledge about EEG, the brain's underlying process, and biometric systems. Methods for extracting relevant information from EEG-signals and the two classification techniques used in this work are also described in this chapter. [1]

2.1 Electroencephalography

EEG is a technique for measuring the brain's electrical activity through different channels. Each channel represents an electrode placed on the scalp. EEG is of relatively low cost, accessible and can easily be managed without special lab setups. This technique provides the ability to analyze brain activity in real-time [14].

The electrodes' placement is specified by the 10-20 electrode placement system devised by the International Federation of Societies for EEG, as shown in fig. 2.1. The system is based on the relationship between an electrode's location and the underlying area of the cerebral cortex [15].

EEG is practiced in hospitals to evaluate several types of neurological diseases, such as epilepsy, tumors, depression, and trauma problems. EEG has also been used for monitoring patients with sleep disorders, and monitor blood flow in the brain during surgical procedures [16, 15]. A computer can translate recorded EEG-signals during a specific cognitive state into desired commands for an external device or the computer itself. Such an application enables people with sensory and motor disabilities to directly control devices and computers via their thoughts, known as Brain-Computer Interface (BCI) [17].

[1] This chapter is an updated version of the background and theory presented in the authors' work described in [13].

One disadvantage of using EEG is the challenge of extracting meaningful information in the time-domain. Raw EEG-signals are nonlinear and non-stationary by nature. The signals are of small amplitudes since they travel through the scalp, skull, skin, and many other layers. EEG-signals acquired non-invasive are, therefore, prone to background noise and artifacts occurring both internally and externally [18]. Regularly occurring artifacts contaminating recorded EEG-signals are muscle movement, blinking, face movements, and external noise like the electrical noise from powerlines.

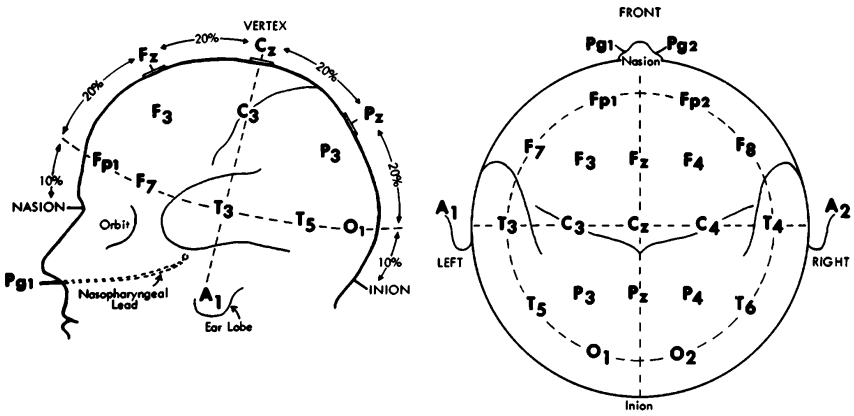

Figure 2.1: Electrode placement according to the international 10-20 system. Left image lateral view, right image top view [19].

2.1.1 How the brain processes information

The neurons (nerve cells) in the brain are what receive, process, and transmit information through electrical and chemical signals. A neuron is built up of a cell body, an axon and several dendrites that branch out of the cell body. The neurons are connected to other neurons by synapses, where neurons receive a potential that produces a movement of ions through the membrane, which creates a current that propagates in the head [20].

The outer portion of the bran is called the cerebral cortex containing about 10^{10} neurons and are strongly interconnected. The processing of information mostly happens in the cerebral cortex. The electrical potential that is measured on the scalp is believed to be generated by the cortex [21]. Current generated by a single neuron is undetectable, a collection of neurons is needed to produce time-dependent electric fields that are measurable using EEG electrodes. Hence, EEG is the measure of the electric potential difference between a reference electrode and a point on the scalp.

2.1.2 Brain frequency bands

Raw EEG data can reveal neural oscillations, which are always a mixture of underlying base frequencies. These base frequencies reflect the different states of the brain that varies depending on individual factors, stimulus properties, and internal states. Brain waves are therefore characterized into the following frequency bands from low to high frequencies: delta, theta, alpha, beta, and gamma bands [22]. The different frequency bands extracted from an EEG-signal is shown in fig. 2.2. These waves are referred to as the frequency bands of the brain. Depending on the brain activity, frequency bands to the specific cognitive process will be active [23]. Frequency bands correlated with their associated mental state is presented in table 2.1.

Brain rhythms	**Frequency [Hz]**	**Description**
Delta	0.5 - 4.0	Deep sleep
Theta	4.0 - 8.0	Memory demands
Alpha	8.0 - 14.0	Awake, relaxed
Beta	14.0 - 30.0	Alertness and focused attention
Gamma	$>$ 30.0	Deep focus

Table 2.1: Brain frequency bands and their respective frequency range [22].

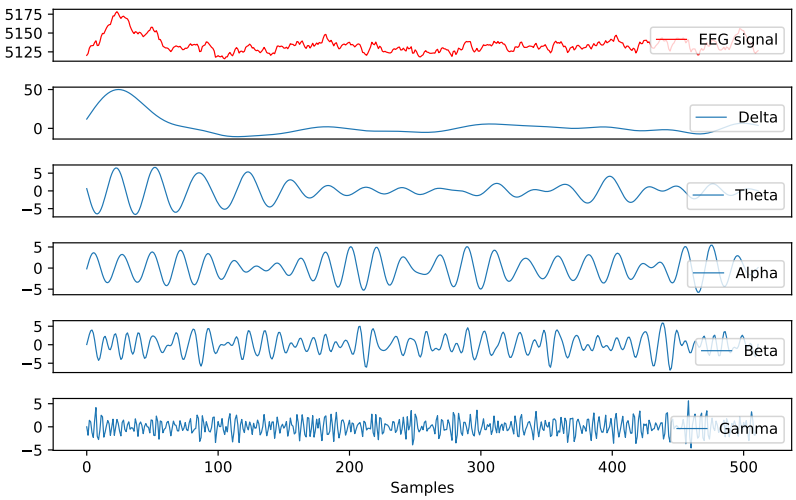

Figure 2.2: Brain frequency bands extracted from an EEG signal.

2.1.3 Event-related potentials

An event-related potential (ERP) is a scalp-recorded voltage fluctuation that is time-locked to an externally defined event [7]. The ERPs are of small voltages and are used to evaluate brain functions and respond to stimuli. A stimulus presented to a subject generates detectable, but time-delayed waves in EEG-signals and indicates how the stimuli are processed according to latency and amplitude [24].

The P3 wave is an essential component in research in the field of ERP. The popular wave pattern P300 occurs approximately 300 ms. after a stimulus is presented, and appears as a series of positive and negative voltage fluctuations in EEG signals [25]. Various paradigms have been used to elicit P300, with the "oddball" paradigm being the most utilized - different stimuli are presented in a series such that one of them occurs relatively infrequently - the oddball. Reduced amplitude in P300 waves can be seen as an indicator of alcohol and drug dependence [24].

2.1.4 Visual evoked potentials

Visual Evoked Potentials (VEPs) are derived from the brain's response to visual stimulation by reflecting the visual information processing mechanism in the brain [26].

2.2 Neuro-paradigms

The brain can be studied by triggering different simulations created by presenting a neuro-paradigm, such as ERP and VEP. ML can be utilized to reveal the recorded EEG-signals containing different patterns obtained by exposing a subject to different neuro-paradigms.

EEG data is collected while the subject rests with their eyes open or closed, or engages in any cognitive task. The acquired EEG data will be different depending on brain activity. It is, therefore, essential to define protocols with neuro-paradigms that will yield brain frequencies of interest. Protocols utilized in EEG-based biometric systems are categorized into two types: resting states and cognitive tasks.

Resting-state paradigm is simple, as the EEG is acquired while the participant is rested during data collection and not performing any particular task. The data can be collected continuously [7].

Cognitive protocols are more complex as the participant engages in some specific tasks while the EEG is acquired. There are many various types of tasks the participant can do and may involve specialized procedures. Participants can engage in mental tasks such as imagining body movements or mathematical operations [27]. EEG can also be acquired while participants are externally stimulated and capture the non-volitional response from the participants. The EEG signals obtained using

a cognitive protocol typically do not rely on the raw EEG time series but on the time-locked ERPs [7]. Other types of stimulation-evoked brain responses used in cognitive protocols are VEP. VEPs are limited to the brain's visual cortex activities. Hence, careful experimental design is required to lower the impact of other brain activities [7].

An advantage of using ERPs over EEG is that EEG-signals are rather unspecific: the state of the participants' brain is unknown, and there is no way to know what the participant is thinking. In contrast, ERPs represents the brain's response to a specific stimulation that is time-locked. This is an advantage in biometric because the results from users are likely to be individuating. A disadvantage of using ERP is that the protocol for acquiring EEG data can be more complex depending on the application. EEG acquired during resting-state requires no stimulation, whereas ERPs can only be acquired while the subject is stimulated in a specific and well-controlled manner [7].

2.3 Biometrics

Biometrics is the technical term for the identification of individuals based on their biological or behavioral characteristics. Any human physiological or behavioral characteristics can be a biometric characteristic as long as the following properties from [28] and [5] are held:

- *Universality*: the characteristic should exist in every individual.
- *Uniqueness*: no other individuals can be equal in terms of the characteristic.
- *Permanence*: the characteristic should be invariant (to the matching criterion) over a period of time.
- *Collectable*: the characteristic can be measured quantitatively.

In terms of practical utilization of a biometric system, other essential requirements need to be considered as well, such as:

- *Performance*: the achievable identification accuracy and speed, the requirement for resources to achieve an acceptable accuracy and speed, and working or environmental factors that affect the identification accuracy and speed.
- *Acceptability*: to what extent are people willing to accept the use of particular biometric characteristic.
- *Circumvention*: how easily the system can be fooled by spoofing or fraudulent techniques.

2.4 Biometric System

A biometric system is a pattern recognition system consisting of acquiring biometric data from an individual, extract a feature set from the acquired data, and compare the extracted feature set against a template set stored in the database [4]. Biometric systems are designed using four main modules as shown in fig. 2.3 [7]:

1. A sensor module capturing the raw biometric data from an individual.

2. A feature extraction module that processes the acquired biometric data to extract a set of features.

3. A matcher module that compares the extracted features during recognition and compares against the stored templates in the database to generate matching scores.

4. A decision making module where user's identity is established (identified) or confirmed (verified) based on matching score.

A biometric system may operate in either identification mode or verification mode depending on the application's context:

- *Identification mode*: the security process of identifying and labeling an individual's identity by searching against a biometric database, to find the distinctive biometric characteristics attribute to a single individual [29]. A one-to-many comparison is conducted by the system to establish an individual's identity without the subject having to claim an identity (*e.g., "Whose biometric data is this?"*) [30].

- *Verification mode*: the security process that verifies an individual's identity by comparing biometric data capture against stored, confirmed authentic data in the database [29]. This is a one-to-one comparison to determine whether the claim is true or not *(e.g., "Does this biometric data belong to Subject 1?")* [30].

This work focuses on the identification mode of an EEG-based biometric system.

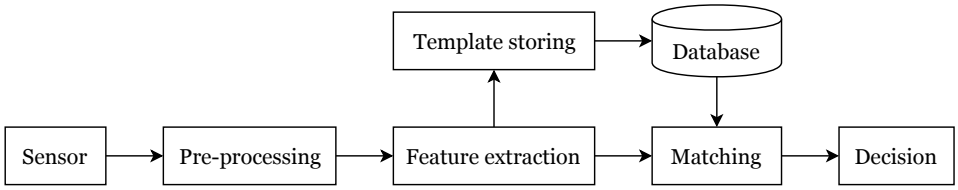

Figure 2.3: Main modules of a biometric system

2.4.1 Brain Biometric Recognition System

Brain biometric systems contain two parts: data acquisition and decision. This applies for both verification and identification applications [7]:

- Data acquisition stage: while the user engages with some protocol, EEG sensors capture electrical brain activity. Data are then transferred for digitization, and the decision-making stage begins.
- Decision-making stage: The collected EEG data are normally contaminated with different kinds of noise, and EEG data have a low SNR. Therefore, the first step is often pre-processing signals to enhance signal quality. Features are then extracted from the signal.

Biometric computation is performed when the feature set has been determined. The biometric computation may be a statistical analysis or complex ML approaches. When authentication is performed, the output will be binary acceptance or rejection. When identification is performed, the output will be the identity label of the user.

Channel Selection and Dimensionality Reduction

Channel selection and dimensionality reduction are often adopted to reduce the computational complexity and dimensionality of EEG data, which normally are large-dimensional [31]. Channel selection also has an additional trait of improving the portability when predicting.

Large data content can contain irrelevant and redundant information, which may degrade the performance of learning algorithms [32]. Moreover, it could result in challenging computational complexity for real-time recognition. Thus, selecting the most relevant data by using features containing most of the information compressed into a lower dimension or using more effective channels are possible solutions [7].

The placement of electrodes on the most effective brain region given a protocol is an effective way to use fewer channels for recording data. However, the selected channels could be unstable or low signal quality due to noise or movement. Adding more channels can, in those cases, provide more reliable and robust data collection [7].

2.5 Signal Analysis Methods

Raw EEG-signals are nonlinear and non-stationary of nature, as mentioned in section 2.1, with added noise and artifacts. Signal analysis is therefore applied to EEG-signals to extract relevant information contained within the signals. Results obtained from the signal analysis will depend on the signal analysis method utilized, the experiment, and the signal characteristics. Hence, several methods are explored.

In biomedical signal processing, such as EEG-signal processing, time-frequency analysis of non-stationary time series data is quite popular. Due to the non-stationary properties of EEG-signals, high resolution in both time and frequency is of interest. This way, any abrupt changes in frequency values for any signal component can be captured in a particular temporal window [33].

EEG has a bandwidth of around 0.5-120.0 Hz, and most of the time, the frequencies of interest are < 30 Hz. Common artifacts such as motion and ocular artifacts appear in the lower frequency region (< 10 Hz) [33]. Thus, high-frequency resolution in the lower frequency region is required.

2.5.1 Fast Fourier Transform

The Fourier Transform (FT) transforms a signal from the time domain to the frequency domain. The signal is represented by sine and cosine functions of unlimited duration. The hidden information in the time domain can be extracted in the frequency domain and analyzed. The Discrete Fourier Transform (DFT) is used when dealing with a finite sequence of equally spaced sampled signals, such as EEG, with the formula defined in Eq. 2.1:

$$X_k = \sum_{n=0}^{N-1} x_n \cdot e^{-\frac{i2\pi}{N}kn} \tag{2.1}$$

where N is the number of complex number $x_n := x_0, x_1 ... x_{N-1}$ transformed into an another sequence of complex number $X_n := X_0, X_1 ... X_{N-1}$. The computational cost of DFT is $\mathcal{O}(N^2)$ where N is the data size. The Fast Fourier Transform (FFT) is therefore used to compute all DFT coefficient as a "block" with a computational cost proportional to $\mathcal{O}(Nlog_2N)$ [34].

The frequency spectrum obtained using the FFT can be used to distinguish the frequency content of components in EEG signals. However, the time information of the signal of what time the specific frequencies appear or disappear will be lost in the frequencies spectrum [35].

2.5.2 Discrete Wavelet Transform

Wavelet transform (WT) replaces the sine and cosine functions of FT by translations and dilations of a window function called *wavelet*. Wavelet is a wave of infinite duration and finite energy correlated with a signal to obtain wavelet coefficients. Wavelets are created from a reference wavelet called the *mother wavelet*, whose coefficients are evaluated for the entire range of translation and dilation factors [36].

The coefficients are evaluated at all instances of time by shifting the mother wavelet continuously along the time scale. The wavelet will then be dilated or scaled to different width and normalized for containing the same amount of energy as the mother wavelet. This process is repeated for the entire signal [36].

Short-time wavelets extract information from high-frequency components in a signal. In contrast, information from low-frequency components is extracted using long-time wavelets. Hence, WT provides well-defined frequency and time resolution for both low and high frequencies. This technique makes WT suitable for analyzing irregular data patterns, such as EEG [37].

There are several methods based on wavelet theory, one of them being the Continuous Wavelet Transform (CWT). The computation for obtaining the CWT coefficient of a signal $x(t)$ with a given mother wavelet Ψ is shown in eq. (2.2)

$$CWT(a,b) = \int_{-\infty}^{\infty} x(t) \frac{1}{\sqrt{|a|}} \Psi(\frac{t-b}{a}) dt \tag{2.2}$$

where a and b are the scaling and shifting parameters, respectively. The calculation of wavelet coefficients on every scale is a computational process and expensive task, which is not suitable for real-time signal analysis. Selecting the scales and shifts based on the power of two will make it much more efficient. This analysis is obtained from DWT defined as

$$DWT(j,k) = \frac{1}{\sqrt{|2^j|}} \int_{-\infty}^{\infty} x(t) \Psi(\frac{t-2^j k}{2^j}) dt \tag{2.3}$$

where 2^j and $2^j k$ replaces a and b, respectively. DWT provides sufficient information of the original signal with a significant reduction in computation time by passing the signal through a series of low-pass and high-pass filter pairs, as illustrated in fig. 2.4.

The first step in DWT is to pass the signal through a low and high-pass filter with the cut-off frequency being the 1/4 of the sampling frequency. According to the Nyquist rule, the output signal holding half frequency bandwidth of the original signal can be downsampled by two [38]. Hence, the frequency resolution is doubled through filtering, and the time resolution is halved through down-sampling at each step [39]. The outputs from the low and high-pass filters are referred to as

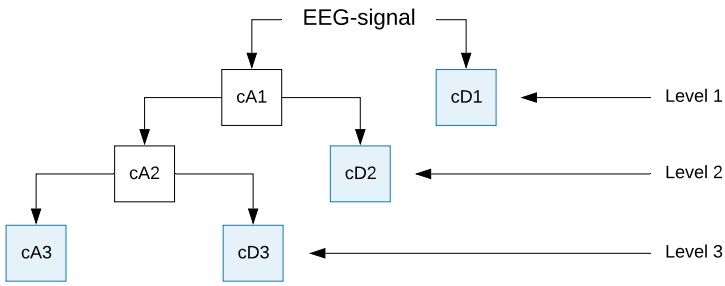

Figure 2.4: Decomposition of an EEG signal using DWT with level 3 decomposition

approximation (A1) and detail (D1) coefficients of the first level, respectively [40]. This step is repeated for the first level approximation and detail coefficient to get the second level coefficients. The process of decomposing EEG-signals results in various frequency bands.

Two parameters must be pre-defined when using DWT: the decomposition level and a mother wavelet. The decomposition of the signal continues until a pre-defined level is reached. The brain frequency bands mentioned in section 2.1.2 can be retained in the wavelet coefficient by defining a suitable decomposition level. The main concept of WT is the similarity of a signal and the selected mother wavelet. Therefore, selecting an appropriate mother wavelet is crucial for analyzing the signals as it will affect the outcome. Finding a mother wavelet resembling EEG-signals' complexity is rather difficult based on visual since EEG-signals do not have a defined signal pattern. An appropriate mother wavelet must be found based on experiments.

2.5.3 Empirical Mode Decomposition

The EMD is an adaptive and data-driven method for decomposing nonlinear, non-stationary, and stochastic processes, such as EEG-signals. This method decomposes a signal into a sum of band-limited functions called Intrinsic Mode Functions (IMFs) without leaving the time domain with defined instantaneous frequencies [41]. Two basic conditions need to be satisfied to be an IMF [42]:

- Condition 1: The number of extrema must be equal, or at most differ by one to the number of zero-crossings.
- Condition 2: At any point, the mean value of the upper and lower envelopes defined by the local maxima and minima must be zero.

The decomposing of signals into IMFs is what makes EMD a data-driven method and does not depend on any *a priori* defined basis system like DWT. IMFs are

extracted through a process called *Sifting*, which removes riding waves and make the wave-profile more symmetric [42] [43]. The sifting process outputs IMFs through an iterative procedure. The flow of the EMD algorithm for generating IMFs is as described in table 2.2.

Input: data sequence x[t]	
1.	Identify all the local extrema in the signal.
2.	Compute lower and upper envelopes from interpolations between extrema; $e_{lower}(t), e_{upper}(t)$
3.	Calculate the local mean value with the lower and upper envelopes; $m_{1,1}(t) = 0.5(e_{lower}(t) + e_{upper}(t))$
4.	Subtract the mean value from the signal; $h_{1,1}(t) = x(t) - m_{1,1}(t)$
5.	Determine if the extracted signal is an IMF with the given conditions of an IMF (Condition 1 and condition 2)
6.	Repeat step 1 - 4 until an IMF is obtained; $c_1(t) = h_{1,k}(t)$
7.	Subtract the obtained IMF from the original signal; $x_2(t) = x(t) - c_1(t)$
8.	Repeat steps 1- 6 until there are no more IMFs to extract. The last component extracted as an IMF is called residual.

Table 2.2: The sifting process in EMD algorithm to generate IMFs.

Once the decomposition of IMFs is finished, the original signal can be reconstructed as

$$x(t) = \sum_{i=1}^{n} c_i(t) + r_n(t) \tag{2.4}$$

A visualization of the sifting process is shown in fig. 2.5. The upper plot illustrates step 1. The middle plot illustrates step 2 - computing upper and lower envelopes after identifying all the local extrema in the signal. The lower plot illustrates the original signal in blue, the averages signal with zero mean in green, and the residual in orange. IMFs extracted from an EEG signal is shown in fig. 2.6

Limitations with EMD

EMD is a data-driven method, meaning IMFs can only be extracted when the signal to be decomposed fulfills the two conditions mentioned in section 2.5.3.

The spline interpolation in the sifting process is an approximation. This approximation leads to a minor deviation from the real mean envelope. End effects occurring nearing the end of a signal are difficulty with EMD and can cause the spline interpolation to produce large swings. A solution for the end effect is presented in [42].

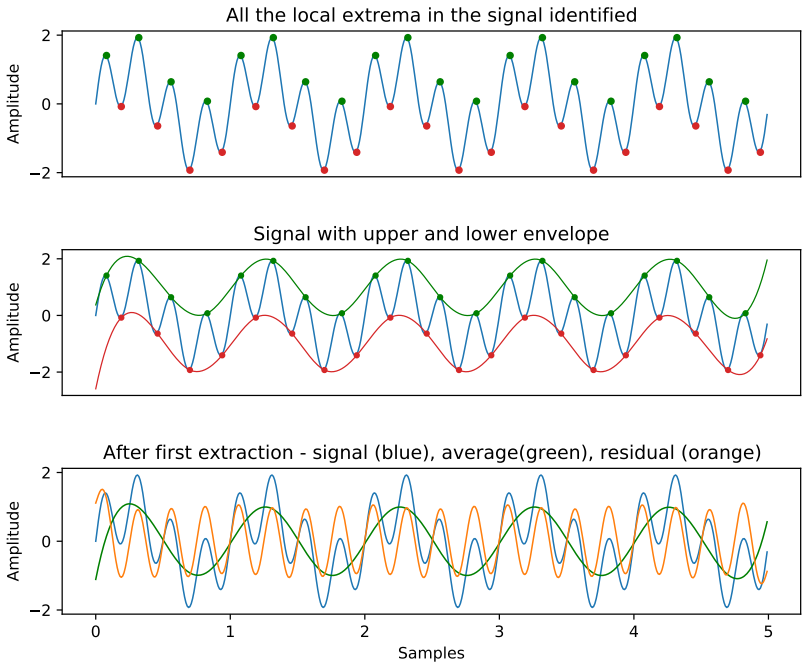

Figure 2.5: Illustration of the shifting process and the spline functions.

Another limitation with EMD is the occurrence of the mode mixing problem during the sifting process. The mode mixing problem occurs when the signal contains intermittency, which can make the IMFs lose their physical meaning. Signal affected by noise can also be the cause of mode mixing, as it can be detected as another kind of intermittency. A solution to this is not focused on this thesis, a method for removing the mode mixing problem is proposed in [44].

Ensemble mode decomposition (EEMD) is a further development of EMD. The EEMD is a more robust method developed since EMD is sensitive to noise, which leads to mode mixing complications. The EEMD defines optimal IMFs components as a means of an ensemble of trials. In each trial, the random noise of finite-amplitude is added to the signal, and EMD is then applied to the new signal. They are thus providing a noise-assisted data analysis. An overall mean is calculated when all trials are finished to obtain the true result [45]. The computational complexity of EEMD is quite heavy due to the ensemble number of trials, which makes is not suitable for real-time applications. As the theory behind EMD is still not complete, it is difficult to predict robustness in EEG recordings and should be taken into consideration [33].

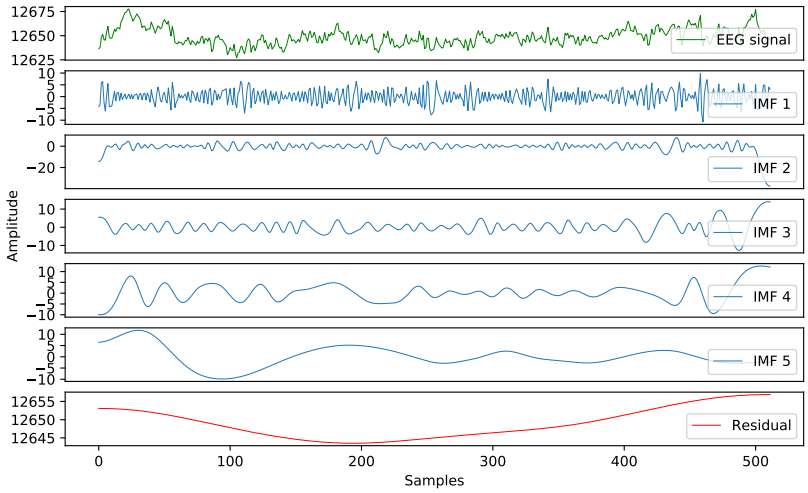

Figure 2.6: Extracted IMFs and residual using EMD on an EEG signal.

2.5.4 Hilbert-Huang Transform

When analyzing nonlinear systems such as brain activity, a proper definition of instantaneous frequency is necessary. Recorded EEG data contains multiple frequencies existing at the same time, which makes instantaneous frequency necessary. One method for achieving this is by the utilization of Hilbert Transform (HT).

Hilbert Transform

The HT generates an analytic signal $z(t)$ by adding the original signal $x(t)$ with the imaginary part of the transformed signal $y(t) = \mathcal{H}\{x(t)\}$ as shown in eq. (2.5)

$$z(t) = x(t) + i \cdot y(t) = a(t)e^{i\phi(t)} \tag{2.5}$$

where

$$a(t) = \sqrt{x^2(t) + y^2(t)} \tag{2.6}$$

$$\phi(t) = \arctan\left(\frac{y(t)}{x(t)}\right) \tag{2.7}$$

$$\omega(t) = \frac{d\phi(t)}{dt} \tag{2.8}$$

represents the instantaneous amplitude, the instantaneous phase, and the instantaneous frequency of the signal, respectively [43]. The purpose of utilizing HT is to obtain local meaningful instantaneous frequencies [42].

Hilbert-Huang Transform

An IMF obtained through EMD represents one of many oscillatory modes in a nonlinear and non-stationary signal, which can be both amplitude and frequency modulated. The obtained IMFs does not represent any good physical interpretation of data on their own and need further analysis.

Taking the HT of a real-valued IMF results in an analytic signal that can be used to extract instantaneous frequency as a function of time. Since the extracted IMFs are obtained from local properties (due to the two conditions for being an IMF), the instantaneous frequency will provide meaningful information about the complex signal. Any event can be localized in both time and frequency axis. The combination of utilizing IMFs from EMD and HT is known as the Hilbert-Huang Transform (HHT) [42].

2.6 Feature Extraction

Feature extraction aims to reduce the number of features in a dataset by creating a new set of features from the existing ones (and then discarding the original features). This can result in improvements in accuracy, overfitting risk reduction, and increase the explainability of a model [46].

A feature represents an individual measurable property of processing being observed [47]. Recorded EEG data contains various features that can be utilized for representing the signals. Classification by using ML learning algorithms can be performed on EEG data by utilizing a set of features. The search for a limited amount of features representing the signal with certainty is a necessary reduction of computation. By understanding the data, the computational requirement can be reduced, remove irrelevant or redundant variables, and improve the predictor performance.

2.6.1 Energy Features

Energy features extract the amplitude and frequency information from the EEG data. The *instantaneous energy* produces information about the signal amplitude and is defined as 2.9

$$f = log_{10}\left(\frac{1}{N}\sum_{i=1}^{N}(S(i))^2\right) \tag{2.9}$$

where $S(i)$ is the coefficient of a signal at position i and N is the length of the signal [48]. The *Teager energy* describes variations in the signal frequency and is obtained with

$$f = log_{10}\left(\frac{1}{N}\sum_{i=1}^{N-1}\left|(S(i))^2 - S(i-1)\cdot S(i+1)\right|\right) \tag{2.10}$$

2.6.2 Fractal Features

The fractal dimension describes how the measure of the length of a curve changes depending on a scale k used as a unit of measurement. A complex index provides the description. Fractal dimension is suitable for signals exhibiting non-stationary and transient characteristics, such as EEG [49]. The *Petrosian fractal dimensions* (PFD) and *Higuchi fractal dimension* (HFD) are two types of fractal dimensions.

The PFD provides a fast computation of the fractal dimension of a signal by translating the series into a binary sequence. The binary sequence is built by assigning a '1' for every difference between consecutive samples in the time series that exceeds a standard deviation magnitude, and a '0' otherwise [50]. The fractal dimension is computed as shown in eq. (2.11)

$$FD_{Petrosian} = \frac{log_{10}n}{log_{10}n + log_{10}\left(\frac{n}{n+0.4N\Delta}\right)} \tag{2.11}$$

where $N\Delta$ is the number of sign changes in the binary sequence, and n is the length of the sequence.

The HFD algorithm calculates the fractal dimension directly from the time series by approximating the mean length of the curve using segments of k samples and estimates the dimension of a time-varying signal directly in the time domain. This results in reduction in running time [51] [52]. The N-sampled data sequence $X(1), X(2), ..., X(N)$ is divided into new time series that are subsets of k samples and are constructed as follows:

$$X_k^m : X(m), X(m+k), X(m+2k), ..., \left(X\left(m + \frac{N-m}{k}\right)k\right) \tag{2.12}$$

where $m = 1, 2, ..., k$ is the initial time and $k = 1, ..., k_{max}$ is the interval time with k_{max} being a constant parameter. In this project $k_{max} = 10$ was used. The length $L_m(k)$ is then calculated for each subset X_k^m as:

$$L_m(k) = \frac{1}{k}\left(\sum_{i=1}^{\frac{N-m}{k}} |x(m+ik) - x(m+(i-1)k)|\right)\left(\frac{N-1}{\frac{N-m}{k}}\right) \tag{2.13}$$

The mean value array for the overall signal is then calculated:

$$L_k = \frac{1}{k}\sum_{m=1}^{1} L_m(k) \tag{2.14}$$

The HFD is estimated using the array of mean values L_k by calculating the least square slope of the trajectory:

$$FD_{Higuchi} = \frac{ln(L_k)}{ln(\frac{1}{k})} \tag{2.15}$$

2.6.3 Statistical Features

Statistical features can be utilized as features for describing EEG data. Table 2.3 describes the statistical features used in this work.

Features	Description
Maximum, Minimum	Highest and lowest potential in a time series
Mean, median	Central tendency, middle score for a set of data arranged in order of magnitude
Variance, standard deviation	Dispersion around the mean

Table 2.3: Statistical features used in this work.

2.6.4 HHT-based Features

Features computed based on HHT are the *marginal frequency* and the *mean instantaneous amplitude*. The former is computed by taking the sum of the instantaneous frequencies from each obtained IMF. The latter is obtained by computing the mean for each IMF. These features are recreated from [53].

2.7 Dimension Reduction

Reducing the dimension for a high-density recorded EEG-signal can reduce the computational complexity when creating a classification model. One method to do so is by using PCA.

2.7.1 Principal Component Analysis

PCA is a statistical technique that reduces the dimensionality of a dataset while preserving as much variability as possible. It reduces the dimensionality of the variable space by representing it with new variables called Principal Components (PCs) that are linear functions of those in the original dataset. The new variables are independent of one another and are calculated, such that the first one explains the highest amount of variability in the system, the second next highest, and so on [33, 54, 55].

PCA highlights specific features of data and reduces the dimension. This is usually a difficult task to identify in the unfiltered spatial data as weights combinations of all EEG channels create the new components. One limitation of PCA utilization is that it fails to separate or identify similar or ocular artifacts from EEG when amplitudes are comparable since PCA depends on the higher-order statistical property [33].

2.8 Multi-class classification

According to [56], ML is a computer's ability to adapt to new circumstances and to detect and extrapolate patterns. Computers can learn from experience using one of two types of learning techniques:

- *Unsupervised learning*: detect hidden patterns from input data.
- *Supervised learning*: use known input and output for training a model to predict future outputs.

2.8.1 Machine Learning

A feature vector created by extracted features and their assigned target labels is used as training parameters for training a model. The model is trained to generate reasonable predictions as a response to new features. This way of training models is known as supervised learning.

A model is trained to predict when new inputs are given with classification algorithms. The unknown target function $y = f(x)$ represents the correct predictions, and the hypothesis function $h(x)$ approximates the unknown target function. The goal of the learning process is to find the hypothesis function that best approximates the unknown target function [56].

Obtaining a hypothesis functions that fit the future data best is of interest. The approximation of a hypothesis function must be tested with unseen data to validate its performance. One method for estimating a trained model's accuracy is by using a method called *k-fold cross validation*. This method first splits the data into k equal subsets and then into training data and test data. Then k rounds of learning rounds are performed. For each round, $\frac{1}{k}$ of the data is used for testing and the remaining for training. The average test score from the k rounds gives a better estimate than a single classifier accuracy score. Most used k values for cross-validation are $k = 5$ and $k = 10$, as they are enough for obtaining estimates statistically likely to be accurate.

In this work, five different ML classification algorithms are utilized for finding the best training model. Descriptions of the classification algorithms used in this work are described below.

Support Vector Machine

A Support Vector Machine (SVM) uses hyperplanes to separate classes of data by maximizing the margins, which are the distance between the nearest training points from different classes [7]. The hyperplane is defined by vectors called support vectors. SVM has an advantage of transforming to higher-dimensional space for easier separation of nonlinear data using kernel trick and is therefore flexible to

represent complex functions [56]. Of the kernels, the linear kernel is computationally efficient. In some cases, it is impossible for the linear hyperplane to separate classes. Therefore, nonlinear decision boundaries are introduced to map data to another space to make them more separable, which increases the classifier's complexity. Examples of nonlinear kernels used are the Radial Basis Function (RBF), sigmoid and polynomial [7].

k-nearest neighbors

The k-NN algorithm does not attempt to construct a general internal model; it stores instances of the training data, so no learning is required. The k-most similar data points to a new data point from the training dataset are localized. A prediction is then obtained by majority voting applied over the k-nearest data points [57]. The learning is based on the k nearest neighbors, where k is an integer value that must be specified by the user. The optimal choice of the value k is highly data-dependent: in general, a large k suppresses the effect of noise but makes the classification boundaries less distinct [58]. The best k-value for the given data can be found by algorithm tuning. The computational complexity of this algorithm increases with the size of the training dataset.

Decision Tree

A Decision Tree (DT) is a non-parametric classifier that predicts the value of the target variable by learning simple decision rules inferred from the data features. DT learning is a heuristic, non-backtracking, one-step lookahead search through the space of all possible decision trees [59]. DT has a structure with each internal node denoting a test on an attribute, each branch representing an outcome of the test, and leaf nodes representing classes or class distribution [60]. The deeper the tree, the more complex decision rules, and the fitter the model. The navigation to the different nodes is test-based, and the output is predicted once the leaf node is reached. The cost of using the tree is logarithmic in the number of data points used to train the tree. A disadvantage of DT is that over-complex trees that do not generalize the data well can be created, called overfitting [61].

Random Forest

The Random Forest (RF) is an ensemble learning algorithm, meaning it generates classifiers and aggregates their results. It consists of several DTs, each giving a prediction, and the class with most votes become the models' prediction. This is a more robust method compared to DT, as this concept protects each of the classifiers from their own individual errors. In an RF, each node is split using the best of a subset of predictors randomly chosen at that node. RF has shown to outperform SVM and k-NN and is robust against overfitting. This is also a user-friendly as it only has two parameters (the number of trees in the forest and the number of variables in the random subset at each node) and is not very sensitive to their values. [62]

Naive Bayes

NB is a probabilistic classifier based on Bayes' Theorem. The simple form of the calculation for Bayes Theorem is as follows:

$$P\left(A|B\right) = \frac{P\left(B|A\right) P(A)}{P(B)} \tag{2.16}$$

where $P(A|B)$ is the probability of interest. The Bayes Theorem assumes that each input variable depends on all other variables, which causes complexity in the calculation. A direct application of the Bayes Theorem becomes intractable as the number of features increases [63].

Removing the assumption of dependency and considering each input variable as independent from each other dramatically simplifies the calculation. The motivation for this concept is the simplification of computation, hence called naive [60]. The fast computing when making decisions is an advantage of NB, and not requiring large amounts of data before learning can begin [64].

2.8.2 Deep Learning

Conventional ML techniques have a limitation of not having the ability to process raw data. The construction of ML systems requires careful engineering and reasonable domain expertise to design a feature extractor that transforms the raw data into a feature vector used as input to a classifier. Using a robust automatic classification of EEG-signals can be an essential step in making EEG more practical in applications and less reliant on human design. Hence, DL is investigated as an additional classification technique in this work [65].

DL is a subset of ML where algorithms inspired by the human brain called Neural Networks (NN) are utilized to learn from a large amount of data. Its called 'deep learning' because of various deep layers in the NN that enable learning [66]. DL has achieved state-of-the-art performance in computer vision and speech recognition, especially with the use of the common deep NN architecture called CNN. It is designed for processing data arranged in sequential arrays of one or more dimensions [67].

Representation learning is a set of methods allowing machines to work with raw data and automatically discover the representations needed for classification. DL methods are representation learning methods containing multiple levels of representation. They are obtained by composing nonlinear modules that transform the representation at one level, into a representation at a higher level. The first level transforms the raw input into a slightly more abstract level. Complex functions, such as EEG, can be learned by obtaining enough of such transformations [67].

For classification tasks, higher layers of representation amplify the input features that are important and suppress irrelevant variations. These layers of features

are learned from data using general-purpose learning procedures, not layers of features designed by human engineers. This is the key aspect of DL. [67].

The objective of NN is to create a model that performs well both on training data and unseen data on which the model will be used to make predictions. The ability to perform well on unseen input data is called generalization. The models' ability to generalize to new data can be estimated using methods like the train-test-split.

Loss is a metric for how a NN learns - by adjusting weights and biases in a manner that reduces the loss. It is of interest to minimize the loss value. In classification, classes are predicted based on probability. Hence loss is also based on probability. The NN minimizes the likelihood of assigning a low probability to the actual class.

Limitations of utilizing deep learning with EEG data

The amount of available EEG data for training compared to image classification is very limited. The collection of EEG data is both time-consuming and physically demanding for the subject performing the experiment. The computational power allows for a classification of EEG data without the need for feature extraction. However, it may not obtain convinced results as the limitation of a small amount of training data [68].

The computation complexity may be much higher using DL than traditional ML, caused by achieving the necessary layers needed for the classification. This is a disadvantage for using DL in real-time applications as more time is needed to train models and may impact the user experience.

When using DL with CNN, interpreting the importance of the features used for classification will be difficult as CNN executes end-to-end learning. The analysis of features used on most traditional ML algorithms is possible but is difficult or impossible with NN. A confusion matrix can be used to assess the performance in greater detail. The accuracy and loss of both training and test sets can also be plotted for each epoch (training rounds) to assess NN's convergence.

Chapter 3

State-of-the-art

Various types of techniques have been carried out to analyze EEG-signals. This chapter gives a summary of the most relevant related work for subject identification using EEG. Most of the related work are offline classification, and two with real-time performance. A summary of state-of-the-art research is presented in table 3.1.

3.1 Classification with feature extraction

Subject identification based on imagined speech as neuro-paradigm was executed in [69]. The EEG-signals were decomposed using EMD, and the most relevant IMFs were selected using the Minkowski distance for each channel. Four features were then computed for each IMF: instantaneous and Teager energy, and HFD, and PFD. The dataset contained 20 subjects imagining 30 repetitions of five words in Spanish in resting-state. The classifiers' RF, SVM, NB, and k-NN were used to compare performance. The 10-fold cross-validation validation gave an accuracy of up to 0.92 using the linear SVM.

An identity authentication system using ERPs as a base was executed in [70]. The dataset consisted of 26 subjects giving a feedback-related response of a P300-speller. Also, in this work, EMD was utilized with Minkowski distance for extracting the most relevant IMFs from each channel. The accuracy index was computed using SVM for classification and the 10-fold cross-validation. A greedy algorithm was used for reducing or increasing the number of channels. The accuracy obtained using nine channels was 0.97 for classifying 24 subjects; the accuracy decreased to 0.91 when only five channels were used.

A study of feature extraction and classification methods were executed in [71]. Three different classification algorithms SVM, k-NN, and NB were employed with two different feature extraction methods EMD and DWT. The aim of the study was subject identification using low-density EEG-signals of resting-state data. A greedy algorithm was used for reducing the number of channels with a minimum

loss of accuracy. The dataset contained recording from 27 subjects using one set with 14 channels and four subsets (8, 4, 2, and 1 channel). EMD showed to be more robust as a technique for feature extraction during resting-state, especially for a low number of channels. The study also showed that linear SVM gives a higher accuracy rate when using high-density EEG-recordings, while Gaussian NB is better for low-density EEG-recordings.

In [72], a four-objective optimisation method for optimal EEG channels selection for detecting intruder as well as identifying subjects was presented. Two IMFs from each channel were extracted using EMD, and two energy features were computed on each IMF. The features were used as input for one-class/multi-class SVM. The method was tested on ERP data collected using 56 channels on 26 subjects. The best result obtained was 0.98 for subject identification, with TAR of 0.96 and True Rejection Rate (TRR) 0.93 using seven EEG channels found using the non-dominated sorting genetic algorithm (NSGA)-III in a subset of subjects manually created.

Feature extraction based on HHT for biometric identification with EEG was performed in [73]. Features computed after taking the HHT of IMFs were instantaneous frequency and instantaneous amplitude. The system was tested on two datasets with different protocols and a single recording channel. The first dataset containing 122 subjects with EEG acquired while users were viewing a series of pictures, and the second dataset contained 109 subjects performing motor and imagery tasks. The instantaneous amplitude-based features were classified using the Linear Discriminant Analysis (LDA) -based classifier. For the instantaneous frequency-based features, the k-NN (3-NN) was used as this gave the best results. The average accuracies obtained from the two datasets using only a single electrode were 0.96 and 0.99, respectively. However, this method must be tested on other paradigms for validation. The first dataset contained only one session, while the second dataset had three sessions separately collected by only a few minutes. An ideal dataset for testing this method is with multiple sessions with intervals of several days to establish stability. In this work, lower frequency bands' utilization seemed to yield better biometric performance for both datasets.

A method for subject identification based on VEP signals and NN was proposed in [74]. A backpropagation NN with a single hidden layer was trained to identify subjects using the gamma frequency band (30-35 Hz) with the spectral power ratio of VEP signals. The dataset included 20 individuals recorded with 61 electrodes. A zero-phase Butterworth digital filter and Parseval's time-frequency equivalence theorem were used to compute the spectral-power ratio of the gamma-band. The NN classification gave an average accuracy of 0.99 across 400 test VEP patterns using a 10-fold cross-validation scheme.

3.1.1 Real-time classification

In [75], the classification of imagined-speech neuro-paradigm was performed intended for real-time classification. DWT with Biorthogonal 2.2 (Bior2.2) as a mother wavelet was used to compute the instantaneous and Teager energy distribution for feature extraction. The Common Average Reference (CAR) was utilized for increasing SNR. For classification, RF classier was implemented with 10-folds cross-validation. The subject identification experiment was conducted on a dataset containing 27 subjects, which imagined 33 repetitions of 5 words in Spanish and obtained an accuracy of 0.98 for subject identification.

A real-time, EEG-based individual identification interface was presented in [76]. The system collected EEG-signals through a mono-polar singe channel in real-time using a mobile EEG device. The interface was evaluated using an experiment involving 20 subjects in resting-state with eyes closed. From the one minute EEG recordings, 27 features in theta (4-7 Hz), alpha (8-13 Hz), and beta (14-30 Hz) bands were extracted as inputs to the classification module. The extracted features were three statistical features (mean absolute amplitude, absolute amplitude, mean square, and variance), Hjorth parameters (activity, mobility, complexity) [77], and three parameters from each frequency bands (max power, center frequency, sum power). The k-NN was utilized for real-time classification. The system gave an accuracy of 1.0 when the system was tested on less than four of 20 subjects and slowly decreased as the number of subjects increased. The accuracy stabilized around 0.7 as the subject capacity increased from 12 to 20.

3.2 Noise reduction and Artifact Correction

Raw EEG-signals usually consist of electrical artifacts, as mentioned in section 2.1. Hence, pre-processing EEG data is crucial for removing or reducing artifacts and noise to improve SNR. The most common of these are the 50 Hz or 60 Hz powerline noise from nearby electronics and muscular artifacts obtained from the movements of the face and eyes.

3.2.1 Artifact Correction: Filtering

Applying filter on raw EEG data is one method for improving SNR. Powerline noise caused by AC power supply can be suppressed by applying a notch filter (bandstop filter) with a narrow stopband at 50 Hz or 60 Hz depending on the AC frequency [7]. The same effect can be achieved by using high or low-pass filtering depending on what frequencies are of interest for the specific experiment.

As mentioned in section 2.1.2, different brain frequency bands can be reflected in EEG data depending on what tasks are executed by a subject. Therefore, by preserving the most meaningful frequency, the SNR can be improved by filtering out the unnecessary brain frequency bands for the given experiment. Various filters can be utilized to keep the most relevant information (e.g., low-pass filters,

band-pass filters) within a specific frequency range. One popular filter for EEG pre-processing is the Butterworth filter because of its flat magnitude in the band-pass [78] [7].

3.2.2 Artifact Correction: Principal Component Analysis

The first few PCs computed by PCA represent most information of the original data. Hence, PCA can be implemented to remove noise by ignoring less important components, in our case number of channels, and reconstruct the input signal using the first few components. This results in increasing of SNR [7] [79]. In [80], PCA was utilized as a pre-processing step for noise reduction and as a feature extraction in [81] [27].

3.3 Deep Learning

The ability to automatically extract relevant features for classification with DL encourages the use of NN in EEG tasks.

CNN was used to automatically extract features and EEG data, and conduct classification for individual identification in [82]. This method was tested on resting-state neuro-paradigm with subjects having their eyes open and closed. The CNN-based identification system yield a high degree accuracy of 0.88 for 10-class classification. Additionally, the inter-personal difference was found using the low-frequency band (0-2 Hz), and obtained results that showed temporal portions at 200 ms. could be used to individualize subjects.

Another paper [83] used CNN for detecting P300 waves in the time domain for BCI. Without any channel selection, the best results obtained for a multi-classifier was a recognition rate of 0.95.

Source	No. Chs.	No. Subj.	Nauro-paradigm	Pre-processing	Artifact removal	Feature extraction method	Features	Classification	Acc.
[69]	14	20	Resting	No	-	EMD	Energy, fractal	RF, NB, SVM, k-NN	0.92
[70]	14, 9	26	ERP	no	no	EMD	Energy, fractal	EMD	0.97
[71]	14, 8, 4, 2, 1	27	Resting	DWT	-	EMD, DWT	Energy, fractal	SVM, k-NN, NB	0.91
[73]	1	122/ 109	ERP	no	no	EMD	Energy, fractal	EMD	0.97
[74]	61	26	ERP	no	no	EMD	Energy, fractal	EMD	0.97
[75]	14	27	Resting	CAR	no	DWT	Energy	RF	0.98
[76]	1	20	Resting	WT, FFT-filter	yes	Theta, Alpha, Beta	Statistical, Hjort, power spec., max power, center frequency sum power	k-NN	0.7
[71]	56	26	ERP	CAR	-	EMD	Energy	one-class multi-class SVM	0.98
[82]	64	10	Resting	normalizing	-	-	-	CNN	0.88
[83]	64	2	ERP	normalizing	-	-	-	CNN	0.95

Table 3.1: Summary of state-of-the-art work.

Chapter 4

Materials and Methods

The following chapter explains the materials and methods used for classifying EEG-signals produced by different neuro-paradigms. The two classification techniques utilized are ML with feature extraction described in section 4.6.1 containing three elements: preprocessing, feature extraction, and classification, and DL described in section 4.6.2 using raw-EEG signals. The methods used for dimension reduction and channel selection are described in section 4.5 and section 4.7, respectively.

4.1 Datasets

In this work, two datasets containing different neuro-paradigms were used for comparing the different classification techniques - both containing subjects in resting-state and executing cognitive tasks.

4.1.1 P300-speller dataset

A dataset from the BCI Challenge, proposed by IEEE Neural Engineering Conference [84] were utilized. The dataset contains EEG data from subjects trying to spell words by paying attention to visual stimuli, known as the "P300-Speller" paradigm. The P300-Speller paradigm uses both EEG and P300-responses to select items displayed on a screen.

The data was recorded from an experiment where each subject was presented numbers and letters to spell words. For selecting a letter of a word, items in a group were flashed on a screen in random order. A letter would then be selected by an online algorithm, which could be either correct or wrong. The subject's feedback response will be a positive or negative feedback-related response of the P300-speller system, lasting for 1.3 *sec*. The recorded EEG-signals are ERPs from positive or negative feedback-related responses of the selected letter. The protocol design using the P300-speller is presented in fig. 4.1.

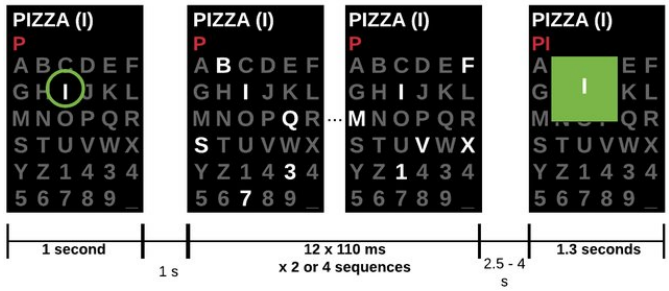

Figure 4.1: Protocol design using P300-speller for recording positive or negative feedback related response [70].

This dataset also contains EEG-signals from subjects at rest lasting for $2.5 - 4\,sec.$ before the selected letter is displayed to subjects, as shown in fig. 4.1. The ERP data containing positive and negative-feedback responses, and the resting-state before the letter chosen by the online algorithm from this dataset are utilized as neuro-paradigms in this work.

The experiment was conducted on 26 subjects (13 male, range $10 - 37$, the mean age of 28.8 ± 5.4 (SD)) with normal or corrected-to-normal vision. EEG data were recorded using 56 passive Ag/AgCl EEG sensors following the extended $10 - 20$ system. Each subject participated in five sessions, with each containing 60 instances with a sampling rate of $200\,Hz$.

4.1.2 Spatial Attention dataset

The second dataset used in the preparation of this work were obtained from the Network - BMI Brain Database Project database (`https://bicr.atr.jp/dbi/download/`). The Network-BMI Brain Database is the result of co-investigators' efforts from the ATR Cognitive Mechanisms Laboratories, Kyoto, Japan. The data was presented at [85, 86].

When collecting this dataset, the subjects were executing spatial attention tasks in which the subjects attended to the right or left following instructions given by the visual stimuli. Each recorded instance consists of two epochs: Attention ($8\,sec.$). and Control ($4\,sec.$). Between each epoch, there are short rest-epochs ($6 - 10\,sec$). The protocol for spatial attention tasks with rest-epoch is shown in fig. 4.2. This rest-epoch was chosen as the second resting-state neuro-paradigm.

The experiment was conducted on 40 subjects between the ages of $20-40$ (mean: 24.6, $SD\,6.4$) with normal or corrected-to-normal vision. The EEG was recorded at a sampling rate of 256 Hz using 64 electrodes referenced to the common mode sense (CMS) active electrode. The EEG channels were placed to cover the whole head on all subjects. Each subject executed one experiment, where each experiment consists of eight sessions, and each session consists of 25 instances.

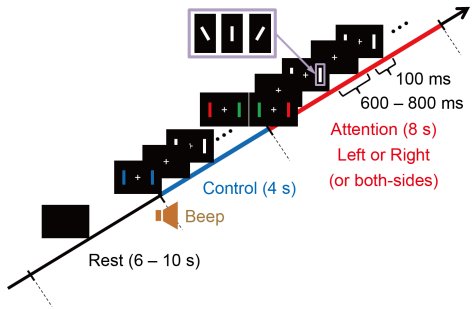

Figure 4.2: Timeline of the Spatial Attention experimental. One instance consisting of 3 epochs: Rest, Control and Attention [85].

Summary of datasets

A summary of the datasets and neuro-paradigms utilized in this work is presented in table 4.1. The different datasets will be referred to as the name given in the table. The resting-state data from Dataset 1 and Dataset 2 are arranged into 2 *sec.* long epochs for the possibility to compare results from the same type of neuro-paradigm acquired from different experiments.

Dataset	Neuo-paradigm	Subjects	Sessions	Instances	Channels	Epoch length
Dataset 1: P300-speller	ERP	26	5	60	56	1.3 sec.
Dataset 1: P300-speller	Resting-state	26	5	60	56	2 sec.
Dataset 2: Spatial Attention	Resting-state	40	8	25	68	2 sec.

Table 4.1: Summary of datasets and neuro-paradigms used in this work.

4.2 Pre-processing

The aim of pre-processing EEG-signals is to improve the SNR. The most relevant information in the raw signals can be obtained by removing or suppressing noise caused by subjects, environment, or electrodes. Analyzing the frequency content of a signal can indicate noise contaminating the signal. Hence, FFT is applied to each neuro-paradigm utilized in this work to analyze the frequency content.

4.2.1 Frequency spectrum of Dataset 1

The frequency spectrum of ERP data and resting-state data from Dataset 1 using raw EEG-signals are shown in fig. 4.3. The EEG-signals are affected by powerline

noise visible at 50 Hz, and 78 Hz with a high-frequency response for ERP and resting-state data. In the experiment where the P300-speller dataset was recorded, a band-pass filter from $1.0 - 20.0$ Hz was used for processing the signals to extract the relevant brain activities from the low-frequency area. Hence, an Infinite impulse response (IIR) Butterworth band-pass filter with $1.0 - 20.0$ Hz of order six was applied to the raw EEG-signals as a pre-processing step. This filter was used because of its maximally flat magnitude in the band-pass [7].

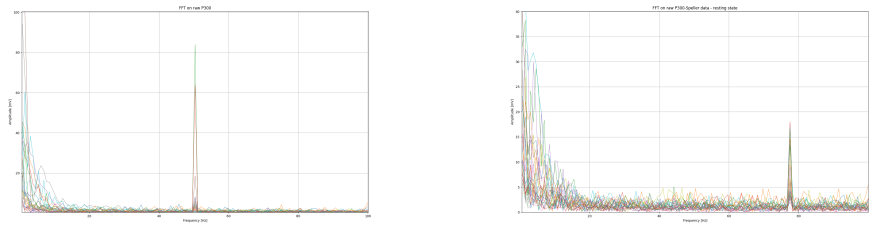

(a) ERP data

(b) Resting-state data

Figure 4.3: Frequency spectrum of raw EEG signals from Dataset 1.

4.2.2 Frequency spectrum of Dataset 2

Fig 4.4 shows the frequency spectrum obtained by taking the FFT of the raw resting-state data from Dataset 2. High-frequency values at 0 Hz caused by offsets in the EEG-signals are visible. There are also visible peaks at 60 Hz caused by the powerline noise. In the experiment where the dataset was recorded, a band-pass filter from $0.5 - 40.0$ Hz was applied to the EEG data to preserve the necessary frequency activity. Hence, The IIR Butterworth band-pass filter with $0.5 - 40.0$ Hz of order six was applied as a pre-processing step for Dataset 2.

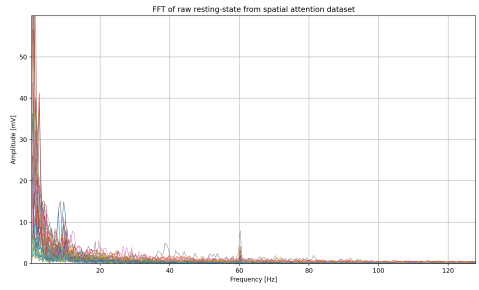

Figure 4.4: Frequency spectrum of raw resting-state data from Dataset 2.

4.2.3 Overview of pre-processing methods

As mentioned in section 3.2, the are numerous ways to pre-processed raw EEG data. As most brain activity exists in the low-frequency range of EEG data, an increase in SNR can be achieved by removing high-frequency components. The signal analysis methods EMD and DWT can improve the SNR by removing the first IMF from EMD or the first coefficient from DWT, as they contain high-frequency mode of a signal. However, depending on the experiment, these components can hold on useful information that can affect the result [87].

There are no defined solutions for this process, as this depends on many factors. Thus, a combination of methods with pre-processing as well as methods without pre-processing, was explored. Regardless, pre-processing is a crucial step for achieving high-quality data. An advanced review of this is out of the scope for this work.

An overview of pre-processing steps used on the methods in this work is presented in fig. 4.5. When using DWT, the first coefficient $D1$ was removed before any feature extraction to remove high-frequency components from the EEG-signals. After band-pass filtering, ERP data, and resting-state data from Dataset 1 contained EEG-signals with a frequency range of $1.0 - 20.0\,Hz$. Hence, only the frequency bands theta, alpha, and beta were included for ERP data and resting-state data from Dataset 1 after pre-processing.

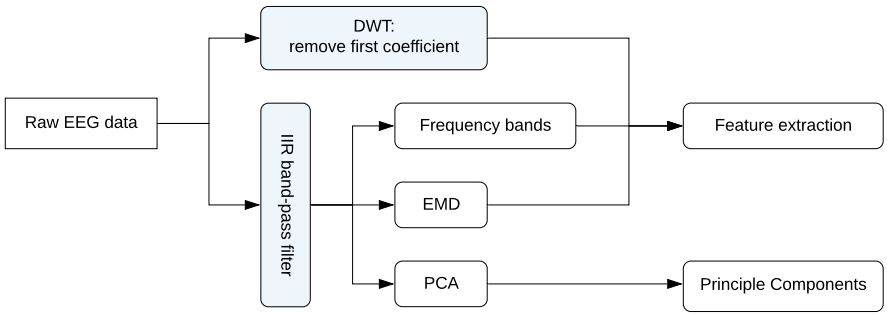

Figure 4.5: Pre-processing steps used on each dataset. For Dataset 1, IIR band-pass filter $1.0 - 20.0\,Hz$ was applied, and for Dataset 2 an IIR band-pass filter $0.5 - 40\,Hz$.

4.3 Decomposition of EEG signals

Two signal analysis methods and filters were utilized for decomposing EEG-signals before any feature extractions: EMD, DWT and, IIR Butterworth band-pass and high-pass filters for extracting brain frequency bands. The effect of employing signal decomposition as a basis for feature extraction will be examined on all neuro-paradigms.

4.3.1 Decomposition with Empirical Mode Decomposition

EMD was applied to each neuro-paradigm data for extracting IMFs from the EEG-signals using a cubic spline function for interpolation. This method was based on experiments from [69, 70, 71].

EMD produces a different number of IMFs depending on the signal content. When training and validating a model using features, it is important to use an equal number of IMFs from each instance when extracting features from IMFs. The most relevant IMFs were therefore chosen using the Minkowski distance as proposed in [88]. For all three neuro-paradigms, the first two IMFs were chosen as this was the minimum number of relevant IMFs in all channels between all subjects. An illustration of decomposing an EEG-signal with n channels using EMD is shown in fig. 4.6.

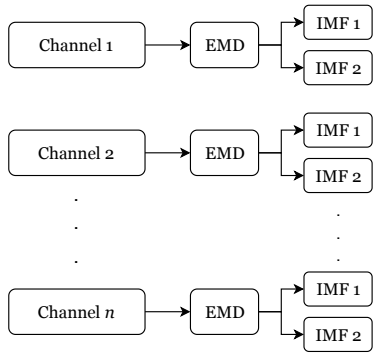

Figure 4.6: EMD applied as a signal decomposition method on n EEG channels.

4.3.2 Decomposition with Discrete Wavelet Transform

DWT was applied to obtain multi-resolution decompositions of EEG-signals. The selection of a suitable mother wavelet is crucial for analyzing the signal using DWT, as it will affect the outcome. Based on related work in [89, 75, 71], the wavelets *Biorthogonal 2.2* (Bior 2.2), *Biorthogonal 4.4* (Bior 4.4), *Symlets 7* (Sym7) and *Symlets 9* (Sym9) were tested as mother wavelets for decomposing EEG-signals. The number on the wavelets represents the order of each wavelet. For Biorthogonal wavelets, the first order is for reconstruction and the second for decomposition.

The wavelet resulting in the highest validation accuracy was chosen as a mother wavelet for the specific neuro-paradigm. An illustration of decomposing an EEG signal using DWT is shown in fig. 4.7.

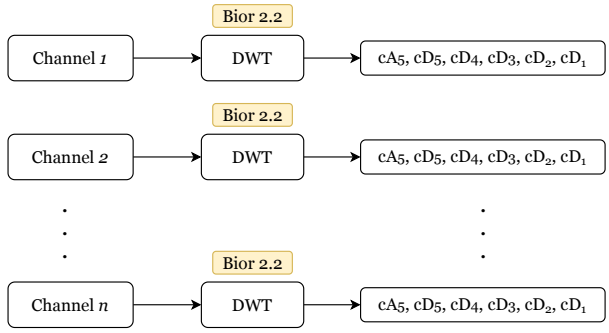

Figure 4.7: DWT with wavelet Bior 2.2 and five levels of decomposition applied as signal decomposition method on n EEG channels.

For all three neuro-paradigms, DWT with five-level decomposition was applied on each EEG channel. The level of decomposition was chosen to resembling the brain frequency bands from section 2.1.2. The frequency bands obtained from each dataset is presented in table 4.2 and table 4.3.

Decomposition Levels	Frequency Bands	Decomposed Signals	EEG Band covered
1	50 - 100 Hz	cD1	Higher Gamma and noise
2	25 - 100 Hz	cD2	Gamma
3	12.5 - 25 Hz	cD3	Beta
4	6 - 12 Hz	cD4	Alpha
5	3 - 6 Hz	cD5	Theta
5	0.5 - 3 Hz	cA5	Delta

Table 4.2: Frequency bands created using DWT with five levels on Dataset 1.

Decomposition Levels	Frequency Bands	Decomposed Signals	EEG Band covered
1	64 - 128 Hz	cD1	Higher Gamma and noise
2	32 - 64 Hz	cD2	Gamma
3	16 - 32 Hz	cD3	Beta
4	8 - 16 Hz	cD4	Alpha (8-14) Hz and Beta (14 - 30)
5	4 - 8 Hz	cD5	Theta
5	0.5 - 4 Hz	cA5	Delta

Table 4.3: Frequency bands created using DWT with five levels on Dataset 2.

4.3.3 Decomposition with frequency bands

With this method, four IIR Butterworth band-pass filters and one high-pass filter were applied on each channel to extract brain frequency bands. Each channel was decomposed into frequency bands: delta, theta, alpha, beta, and gamma with their corresponding frequencies described in table 2.1. An illustration of signal decomposition using frequency bands is illustrated in fig. 4.8.

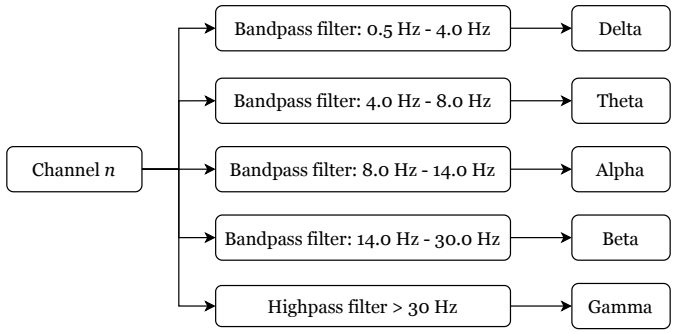

Figure 4.8: Decomposing each EEG channel into frequency bands.

4.4 Feature extraction

Once the EEG-signals were decomposed, features were extracted. The features presented in table 4.4 were extracted from all three neuro-paradigms.

Feature type	Extracted features
Energy	instantaneous energy and teager energy
Fractal	petrosian and higuchi fractal dimension
HHT-based	marginal frequency, mean instantaneous amplitude
Statistical	min, max, mean, median, variance, standard deviation

Table 4.4: Features extracted from Dataset 1 and Dataset 2.

The behavior of feature combinations on the different neuro-paradigms is of interest. Table 4.5 shows the different feature sets used in this work.

Feature sets	1	2	3	4	5	6
Feature types	energy	statistical	HHT-based	energy, fractal	energy, fractal, statistical	energy, fractal statistical, HHT-based

Table 4.5: Features sets used after decomposition.

4.5 Dimension Reduction

PCA minimizes the number of variables used to explain the maximum variance for a given dataset. PCs obtained from applying PCA on each epoch were used to create a feature vector. The feature vector was then utilized as input to the ML algorithms for creating classification models.

The number of PCs obtained is based on the cumulative variance in a dataset. PCA allows us to observe the trade-offs between the number of PCs utilized and the total variance explained by the data. For instance, fig. 4.9 presents the fraction of variance explained by each PC using ERP data from Dataset 1. A threshold at 95% is marked to show how many PCs are needed to preserve 95% of the total variance in the dataset.

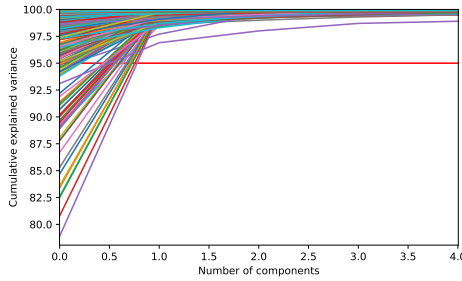

Figure 4.9: Cumulative explained variance for all epochs using ERP data from Dataset 1. The red line marks 0.95 of the total variance.

The number of PCs obtained varies on each epoch individually. To create feature vectors of equal length, an equal number of PCs must be extracted from all epochs. The smallest number possible was chosen considering efficiency and performance. For all three neuro-paradigms, the two first PCs were enough for retaining 95% of the variance representing the original data. ERP data using 56 channels with 2 PCs gave a feature vector of length: $channel \times nPC = 56 \times 2 = 112$. Figure fig. 4.10 illustrate the process of using PCA as a dimension reduction technique with classification.

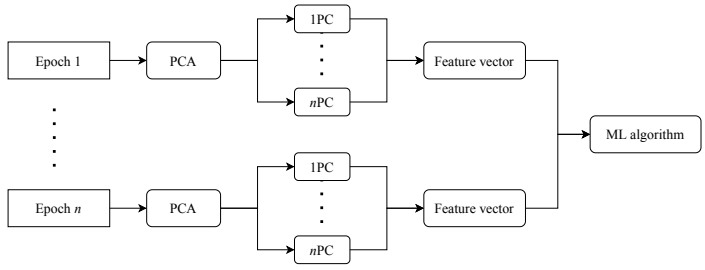

Figure 4.10: PCA applied on epochs for obtaining PCs to create feature vectors.

4.6 Classification

Two different techniques were utilized in the classification part as illustrated in fig. 4.11. The first classification technique uses feature extraction and ML classification algorithms explained in section 4.6.1, while the second technique uses DL to classify raw EEG-signals as explained in section 2.8.1.

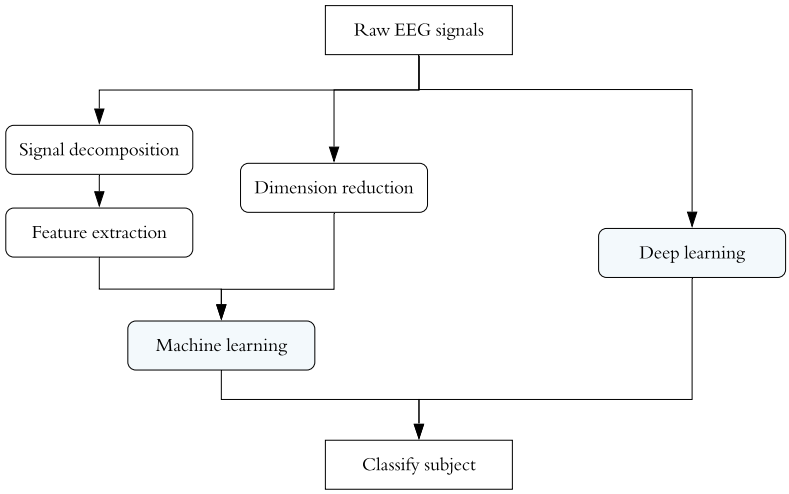

Figure 4.11: Flowchart of classification techniques used in this work.

4.6.1 Classification using feature sets

An overview of the signal decomposition methods, features, and classification used on each neuro-paradigm for obtaining accuracy is described in four steps (far left branch in fig. 4.11):

1. *Decompose the individual EEG-signals*

EEG-signals were decomposed using EMD (two IMFs), DWT (five frequency bands), and IIR Butterworth filters (five brain frequency bands) separately. The EMD algorithm utilized in this work is from the PyEMD package [90]. The DWT algorithm is from the PyWavelet package [91], a free Open Source software. The IIR Butterworth band-pass and high-pass filters used in this work were created using the open-source Python Scipy Signal processing package [92].

2. *Create an array of features for each decomposition*

For each decomposed signal, feature sets presented in table 4.5 were computed, and an array of features for each channel in an EEG-signal was created. This process was performed on each neuro-paradigm using EMD, DWT, and frequency bands as a basis for feature extraction.

3. *Clasify the feature vectors and obtain accuracy for each classefier*

The obtained arrays of features from each channel were then concatenated to obtain a single feature vector per instance. The created feature vectors were used as input to the classifiers. Figure 4.12 shows an illustration for obtaining a feature vector from an instance using EMD as a basis for feature extraction. The feature vector's size varied depending on what features were extracted and the method used for decomposing the signals. E.g., an instance containing five channels with EMD as basis function for extracting statistical features would result in a feature vector of size 60 ($channels \times IMFs \times features = 5 \times 2 \times 6 = 60$).

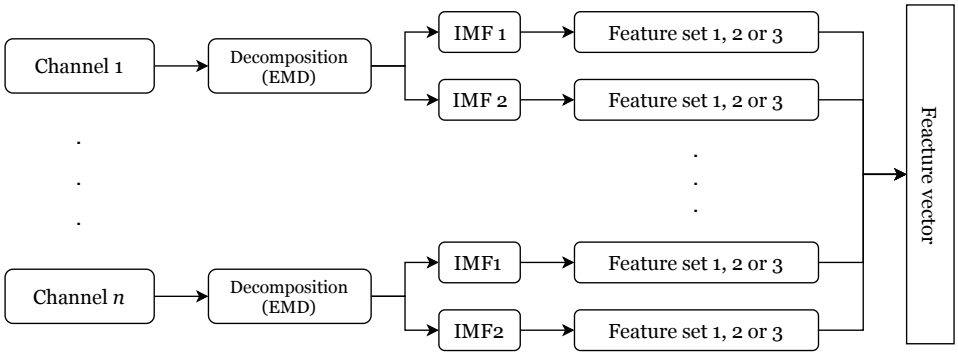

Figure 4.12: Illustration of creating a feature vector for an instance using EMD as basis for extracting features. Feature extracted from each EEG channel is concatenated to create one feature vector.

4. *Select classifier model with the highest accuracy*

Supervised ML models were created using the 5-fold cross-validation for obtaining the model accuracy. The ML algorithms used for creating models were: DT, RF, k-NN, SVM, and NB. The best parameter for each classifier was found by repeating experiments using different parameters and select the classifier with the highest accuracy. The set of parameters used for each classifier was based on work in [13]:

1. RF: depths = [2, 3, 4, 5, 6]
2. k-NN: neighbors = [2, 3, 4, 5, 6, 7, 8, 9, 10]
3. SVM: kernels = [linear, radial basis function (RBF), sigmoid polynomial]

The classifications algorithms used in this work are from Scikit-learn [93], an open-source machine learning library in Python containing several built-in classification algorithms. The GaussionNB from the Sckit-learn library was used for getting the NB classifier with its default parameters.

4.6.2 Classification using deep learning

The second classification technique (right branch in fig. 4.11) uses raw EEG-signals (voltage) as input for a CNN. The CNN architecture implemented in this work was based on a public architecture called EEGNet [94]. The model was designed for classifying raw EEG data. EEGNet was made with the goals of i) be applied across several different BCI paradigms, ii) be trained with minimal data, and iii) produce neurophysiologically interpretable features. Figure 4.13 visualizes the EEGNet architecture and shows the four main sections after input.

The first sections (Conv2D) executes a convolution with several temporal filters, within each channel, with a size of half the sampling rate. The convolutions result in a series of signals bandpass-filtered of different sizes.

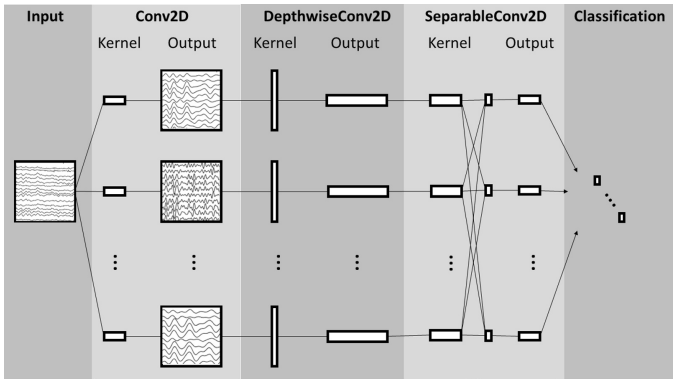

Figure 4.13: Illustration of EEGNet architecture [94].

The second section (DepthwiseConv2D) uses the previous layer's output to perform a depth-wise convolution, which results in frequency-specific spatial features by extracting spatial features (between channels) from each temporal filter. This step allows for extracting meaningful features from EEG-signals. Depth-wise convolution reduces the number of trainable parameters to fit.

The third section (SeparableConv2D) is a combination of depth-wise convolution, followed by a point-wise convolution. This step summarizes and combines the output from the previous layer in a meaningful way. The benefits of using separable convolutions are reducing the number of parameters to fit and optimally merging the outputs.

The last section is the final classification by a softmax layer. This CNN architecture allows extracting essential features from raw EEG-signals while limiting the number of interest parameters.

4.7 Channel Reduction

Using a large number of channels in EEG recordings in real-time classification will make the system computationally expensive. In [70], it was found that a subset of five channels was enough for giving a high accuracy rate comparable with the accuracy obtained using all channels. In this work, five channels from each neuro-paradigm were selected for testing the classification techniques with a reduced number of channels.

The channels were chosen based on work in [95], where five channels were chosen for EEG Seizure Detection. The channel with the lowest standard deviation (SD) was first selected with the idea of low SD when seizures are detected and high SD when noise and muscular artifacts are present in EEG-signals. The remaining four channels were then selected based on the similarity of the first selected channel. The mutual information (MI) was used as a quantitative measure for finding the similarity of two random variables and were applied for finding the interdependent channels with the first selected channel. The four remaining channels selected resulted in higher MI than the first channel.

The main reason for using fewer channels is to reduce the computational complexity for real-time classification using low-density EEG recording. However, channel selection can also provide channels that contain more information for the neuro-paradigm used.

Chapter 5

Experiment design and implementation

This chapter explains the implementation of a simulated subject identification system for real-time classification. The server and database used in this work are part of the EEG-based biometric system containing both identification and authentification layer as described in chapter 1.

5.1 Server API for EEG-based Biometric System

To use the biometric system in real-time, a Representational State Transfer (REST) Application Programming Interface (API) was created using *Django* with Python 3.7. Django is a free and open-source high-level Python web framework for building Web Applications, and it is a popular server-side web framework [96].

The REST API created with Django contains five apps with different functionalities: commonApp, subject, data, identification, and authentication. For the identification layer, all the apps except for authentication were utilized.

5.1.1 Server-side endpoints

All requests sent to the server for handling the data were made using the HTTP POST method. The POST method is used for sending data to the server to create or update the server resource. POST requests have no restrictions on the data length, which is important for sending recorded EEG-signals to the server for further processing. All requests sent to the server will modify the server resource, making the HTTP POST method a suitable HTTP method for sending requests to all the endpoints.

The four endpoints used for the identification part of the system is presented in table 5.1. The first endpoint *eeg/subject/add* saves the subject information in the system. The second endpoint *eeg/data/save* stores the recorded EEG-signals in the database. The third endpoint *eeg/identification/training* trains a classification model and stores the trained model in the database. The last endpoint *eeg/identification/identity* is used to predict the identity of the user. The API documentation of all endpoints, including authentification, created for the biometric system is presented in chapter C.

URL	HTTP method	Data
eeg/subject/add	POST	application_id, name
eeg/data/save	POST	application_id, feature_type, data = {data, target}
eeg/identification/training	POST	application, feature_type, classifier
eeg/identification/identify	POST	application_id, instance

Table 5.1: Endpoints used for identification layer of the biometric system.

5.1.2 Database Design

The models created per task and experiments must be stored in a database when using the system in real-time. A database was created using MySQL, an open-source relational database management system. The database consists of several tables made up of columns (fields) and rows (records). The database is primarily responsible for storing information organized in tables and their relationship with each other.

The database was created for storing subject information, EEG data from subjects, and the trained models used for identification and authentication. The tables used for creating the database are described with an Entity-Relation diagram showing the relations between the different tables in fig. 5.1. The tables relevant to the identification layer are described below.

applications

The applications table gives the possibility to create multiple applications that can be used for different purposes. The application can represent the name of an organization using the system or create separate environments for testing and production. The application table must be defined before identification can start as the other tables created will be connected to the application table. The other tables in the database hold a Foreign Key (FK) referencing the application tables Primary Key (PK).

subjects

The subject's name is stored in the subjects table. The table is connected to the application table with an FK representing the application id. More variables like age and sex of the subject can be added if needed.

instances

Recorded EEG-signals need to be stored when adding a new subject to the system. To ensure the given EEG-signals are not stored in the database without an owner, the instances table has an FK representing the PK in the subject table equaling the subject id. This table stores recorded raw EEG-signals and features extracted from the signals when adding a new subject to the system. The stored data is then used for training a model.

catalogs

The catalogs table stores trained models to be used when predicting a subject. When predicting a subject, the last trained model stored in the table is used. The catalogs table is connected to the application table with an FK representing the application id.

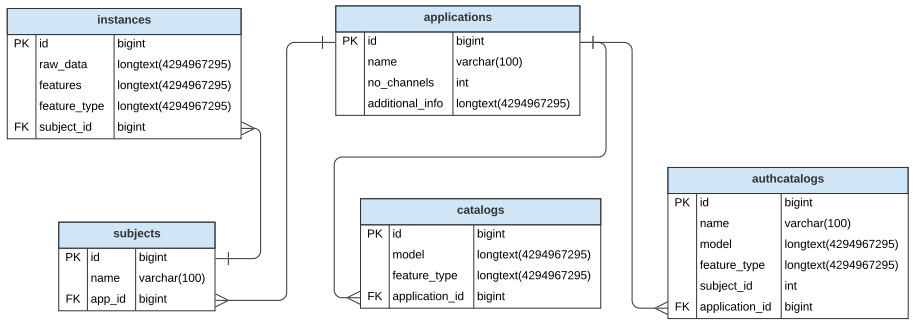

Figure 5.1: Entity-Relation Diagram of database used in EEG-based Biometric System.

5.2 Simulated Subject Identification System

The simulated system was created based on results obtained from the methods presented in chapter 5 in offline-classification—the classification technique most suitable for the real-time classification was used for creating the system. The final implementation is presented in section 6.4, after discussion of offline classification.

Chapter 6

Results and Discussion

The following chapter presents results obtained from offline and real-time classification. The first part of this chapter presents results obtained from an offline classification using methods described in chapter 5. The second part presents results from the simulated real-time experiment created using the best classification technique from offline-results. Discussion of offline and real-time classification is presented in section 6.3 and section 6.5, respectively.

6.1 Offline classification using machine learning

Finding an optimal combination of methods for creating an ML classification model with high accuracy and performance is of interest. The following experiments are proposed:

1. Classification using all methods separately on each neuro-paradigm with EEG-recordings containing all channels.
2. Classification using all methods separately on each neuro-paradigm with EEG-recording containing five channels.

The experiments aim to investigate which classification algorithms with given features and signal decomposition or dimension reduction, results in the highest accuracy for low- and high-density EEG-recordings on different neuro-paradigms. The experiments also address the first research question presented in chapter 1, by testing the same methods on different datasets containing the same type of neuro-paradigm. All the experiments in this section followed the procedures described in section 4.6.1 and section 4.5.

The created classification models were trained using EEG data from session 1, using five instances per subject. The trained model with the highest accuracy was then validated on unseen EEG data from session 2. This was applied for each neuro-paradigm data. This setup of only using one session for training with few

instances was done to resemble a real-world application. Training the ML models with multiple sessions is ideal for creating a robust classification model. However, in real-life, this will be an exhausting process for the subject to be identified. The presented validation accuracy was obtained using the 5-fold cross-validation. Each dataset has balanced classes making accuracy a suitable metric for assessing the performance.

The results presented in this section contain validation accuracy from all three signal decomposition methods (EMD, DWT, frequency bands) and dimension reduction (PCA) with and without pre-processing. The feature set resulting in the highest validation accuracy for the specific method is presented. For PCA, the number of PCs used is presented.

The different methods with their best feature sets are compared to determine the most suitable combination of methods for the given neuro-paradigm, based on performance and validating accuracy. The performance of the different methods with their feature set is observed by testing them on different amounts of subjects. Each model was created using 20 %, 40 %, 60 %, 80 % and 100 % of the subjects from each dataset.

6.1.1 Machine learning classification using all channels

The neuro-paradigms described in table 4.1 were tested using all channels from each EEG recording to observe the performance of using high-density EEG recordings.

Results from using ERP data from Dataset 1

The validation accuracies obtained using ERP data from Dataset 1 are presented in table 6.1, and the performance of each method is presented as graphical line plots in fig. 6.1. Using raw EEG data, PCA with 2 PCs gave high accuracy when using few subjects but rapidly decayed in accuracy when the number of subjects increased. When using the complete dataset (100%), the highest validation accuracy of 0.74 was obtained using frequency bands with energy features and EMD with energy and statistical features on raw EEG data. Frequency bands show higher average accuracy than EMD, which results in frequency bands having better overall performance than EMD. Of all the methods, DWT with mother wavelet Sym7 and statistical features using raw EEG data had the most stable performance, but lower average validation accuracy than frequency bands. For all the methods, higher validation accuracy was obtained with raw EEG compared to using pre-processed EEG data.

The ML algorithms used for creating classification models and obtaining validation accuracy varies for each method used and the number of subjects, as shown in, table 6.1. The performance of all five classifiers (RF, DT, k-NN, SVM, and NB) used with frequency bands and energy features on raw EEG data is presented in fig. 6.2. For all classifiers, the accuracy performance varies as the number of

subjects increases. DT has an oscillating performance, while k-NN decreases in accuracy with no stable performance as the number of subjects increases. The performance of each classifier used depends on the method and features used for training the models. Testing all features and methods with different classifiers is necessary to obtain the highest validation accuracy possible and is performed on all experiments in this section.

Data	**Method**	**Features**	**Number of subjects in percentage (Total: 26 subjects)**				
			20 %	**40 %**	**60 %**	**80 %**	**100 %**
Raw	EMD	Energy, Fractal	2-NN:	RF-5:	2-NN:	2-NN:	RF-5:
		Statistical	0.800	0.880	0.750	0.705	0.739
	DWT	Sym 7	RF-2:	RF-2:	RF-2:	RF-4:	RF-4:
		Statistical	0.800	0.700	0.675	0.648	0.654
	frequency bands	Energy,	RF-2:	RF-5:	RF-5:	RF-4:	RF-6:
		Fractal	0.880	0.880	0.825	0.708	0.739
	PCA	2 PC	RF-2:	RF-2:	RF-4:	RF-2:	RF-4:
			1.000	0.940	0.850	0.676	0.584
Pre-processed	EMD	Energy	linear SVM:	linear SVM:	linear SVM:	linear SVM:	RF-5:
			0.760	0.520	0.538	0.476	0.5077
	DWT	Sym 7	RF-2:	RF-2:	RF-3:	RF-5:	Rf-5:
		Statistical	0.760	0.620	0.613	0.610	0.654
	frequency bands	Energy,	7-NN:	linear SVM:	RF-6:	RF-5:	RF-6:
		Fractal	0.680	0.680	0.625	0.467	0.423
	PCA	1 PC	linear SVM:	linear SVM:	linear SVM:	linear SVM:	linear SVM:
			0.880	0.844	0.713	0.629	0.533

Table 6.1: Validation of ERP data from Dataset 1 using raw and processed EEG-signals containing 56 channels. Models were trained using session 1 and validated on session 2.

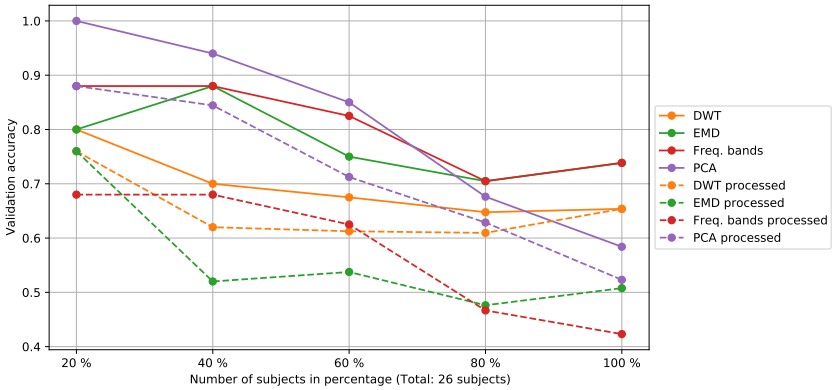

Figure 6.1: The evolution of validation accuracy of ERP data from Dataset 1 using raw and processed with EEG-signals containing 56 channels. Models were trained using session 1 and validated using session 2.

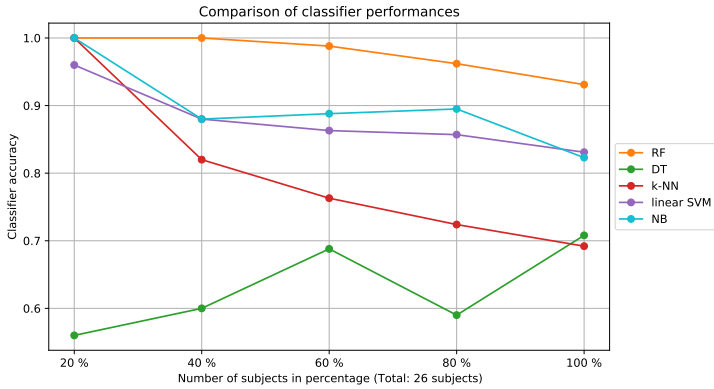

Figure 6.2: The evolution of accuracy obtained using ML algorithms (RF, DT, k-NN, linear SVM, and NB) with frequency bands as a basis for extracting energy features using ERP data from Dataset 1.

Results from using resting-state data from Dataset 1

The results from using resting-state data from Dataset 1 is presented in table 6.2 and plots of the performances in fig. 6.3. PCA with 2 PCs on raw EEG data resulted in high validation accuracy when less than 60% of the dataset was used and decreased in accuracy as the number of subjects increased. When testing the full dataset (100%), the highest validation accuracy of 0.74 was obtained using frequency bands with energy features on raw EEG data. Frequency bands had a stable validation accuracy of 0.84 when 60% of the dataset was tested. The performance of EMD with statistical features on raw EEG data became more stable as the number of subjects increased, but with an overall validation accuracy lower than frequency bands. DWT using mother wavelet Bior2.2 with energy features on raw EEG data resulted in the lowest average validation accuracy for this neuro-paradigm. When 20% of the dataset was used, pre-processed EEG data resulted in higher validation accuracy for EMD, frequency bands, and DWT than using raw EEG data. When a higher percentage of the dataset was used, better accuracy was achieved using raw EEG data. Overall higher performance was obtained using raw EEG data for all the methods.

Results from using resting-state data from Dataset 2

Results from using the resting-state data from Dataset 2 dataset is presented in table 6.3 and plots of the performance in fig. 6.4. DWT using mother wavelet Bior2.2 and energy features, and PCA with 2 PCs on raw EEG data gave high validation accuracy when less than 80% of the dataset was used. As the number of subjects increased, the DWT performance remained stable, while PCA decreased in accuracy when the full dataset (100%) was tested. EMD and frequency bands with energy features had the same performance and validation accuracy when tested on

60% of the dataset on raw EEG data, and decreased in accuracy as the number of subjects increased. The highest validation accuracy of 1.00 was obtained using DWT with mother wavelet Sym7 and energy features on pre-processed EEG data. For the other methods, higher validation accuracy was obtained using raw EEG data compared to pre-processed EEG data.

Data	**Method**	**Features**	**Number of subjects in percentage (Total: 26 subjects)**				
			20 %	**40 %**	**60 %**	**80 %**	**100 %**
Raw	EMD	Statistical	RF-2: 0.520	2-NN: 0.800	2-NN: 0.750	2-NN: 0.714	linear SVM: 0.7154
	DWT	Bior 2.2 Energy	RF-2: 0.600	2-NN: 0.740	2-NN: 0.738	linear SVM: 0.6571	linear SVM: 0.577
	frequency bands	Energy, Fractal	4-NN: 0.840	RF-4: 0.838	RF-5: 0.838	RF-5: 0.752	RF-6: 0.739
	PCA	2 PC	RF-2: 1.000	RF-2: 0.960	RF-2: 0.838	RF-4: 0.752	RF-3: 0.672
Pre-processed	EMD	Energy, Fractal	linear SVM: 0.960	linear SVM: 0.700	linear SVM: 0.713	linear SVM: 0.619	RF-5: 0.508
	DWT	Bior 2.2 Energy	RF-2: 0.680	RF-2: 0.740	RF-5: 0.638	linear SVM: 0.6381	linear SVM: 0.577
	frequency bands	Statistical	linear SVM: 1.000	linear SVM: 0.755	linear SVM: 0.775	linear SVM: 0.667	linear SVM: 0.592
	PCA	2 PC	4-NN: 0.960	linear SVM: 0.689	linear SVM: 0.838	linear SVM: 0.752	RF-5: 0.492

Table 6.2: Validation of resting-state data from Dataset 1 using raw and processed EEG-signals containing 56 channels. Models were trained using session 1 and validated using session 2.

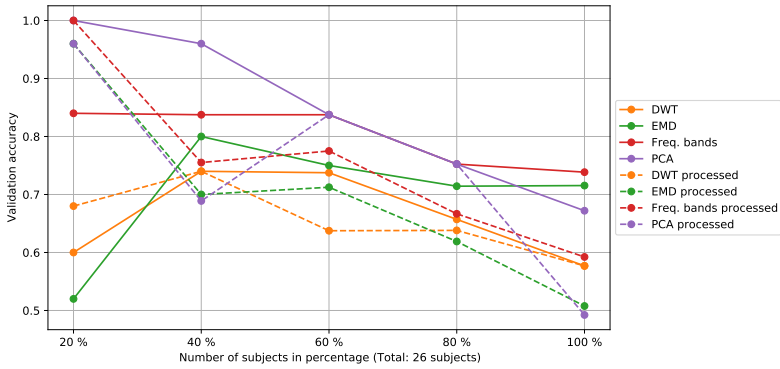

Figure 6.3: The evolution of validation accuracy of resting-state data from Dataset 1 using raw and processed EEG-signals containing 56 channels. Models were trained using session 1 and validated using session 2.

Data	Method	Features	Number of subjects in percentage (Total: 40 subjects)				
			20 %	**40 %**	**60 %**	**80 %**	**100 %**
Raw	EMD	Energy, Fractal	RF-2: 0.8000	linear SVM: 0.825	linear SVM: 0.738	linear SVM: 0.575	linear SVM: 0.565
	DWT	Bior 2.2 Energy	RF-2: 0.875	RF-2: 0.888	linear SVM: 0.992	linear SVM: 0.975	linear SVM: 0.980
	frequency bands	Energy, Fractal	RF-2: 0.825	linear SVM: 0.813	linear SVM: 0.742	linear SVM: 0.688	linear SVM: 0.665
	PCA	2 PC	linear SVM: 1.000	2-NN: 0.938	2-NN: 0.917	2-NN: 0.906	RF-5: 0.672
Pre-processed	EMD	Energy, Fractal	linear SVM: 0.750	linear SVM: 0.738	linear SVM: 0.600	linear SVM: 0.575	linear SVM: 0.575
	DWT	Sym 7 Energy	RF-2: 1.000	RF-2: 0.988	2-NN: 0.992	2-NN: 0.994	2-NN: 0.995
	frequency bands	Energy, Fractal	RF-3: 0.825	linear SVM: 0.788	linear SVM: 0.675	linear SVM: 0.638	linear SVM: 0.615
	PCA	1 PC	linear SVM: 0.675	RF-4: 0.463	linear SVM: 0.508	linear SVM: 0.475	linear SVM: 0.475

Table 6.3: Validation of resting-state data from Dataset 2 using raw and processed EEG-signals containing 56 channels. Models were trained using session 1 and validated using session 2.

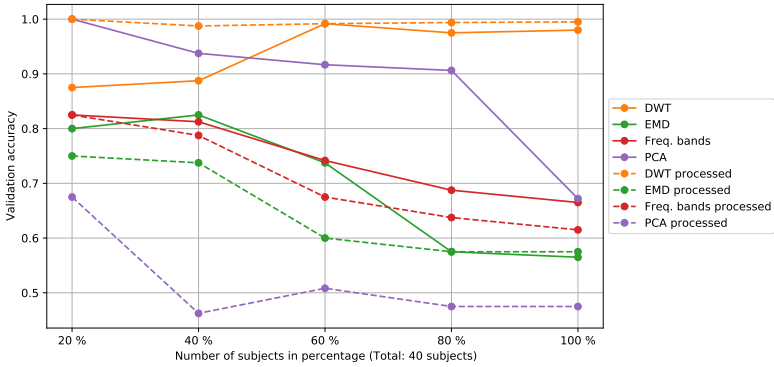

Figure 6.4: The evolution of validation accuracy of resting-state data from Dataset 2 using raw and processed with EEG-signals containing 68 channels. Models were trained using session 1 and validated using session 2.

6.1.2 Machine learning classification with channel reduction

The methods from chapter 5 were tested using EEG-recordings containing five channels on each neuro-paradigm. The channels were found using the method described in section 4.7 and are presented in table 6.4.

Dataset	Neuro-paradigm	Channels
Dataset 1: P300-speller	ERP	[1, 31, 32, 33, 42]
Dataset 1: P300-speller	Resting-state	[1, 31, 32, 33, 42]
Dataset 2: Spatial Attention	Resting-state	[1, 21, 37, 38, 39]

Table 6.4: The five channels selected for each neuro-paradigm.

Results from using ERP data from Dataset 1

The results from using ERP data from Dataset 1 are presented in table 6.5 and as a graphical line plot in fig. 6.5. The validation accuracy decreased for all methods when 40% of the dataset was used and then stabilized as the number of subjects increased. This was the case when using both raw and pre-processed EEG data. When testing the complete dataset (100%), the highest validation accuracy of 0.42 was obtained using frequency bands with energy features on raw EEG data. DWT using mother wavelet Bior4.4 with statistical features gave higher validation accuracy using pre-processed EEG data compared to raw EEG data. The rest of the methods resulted in lower validation accuracy when using pre-processing EEG data.

Results from using resting-state data from Dataset 1

The validation accuracy for resting-state data from Dataset 1 is presented in table 6.6 and plots of the performance in fig. 6.6. The highest validation accuracy of 0.64 was obtained using DWT with mother wavelet Bior2.2 and energy features on pre-processed EEG data, with volatile performance. The second highest validation accuracy 0.48 was obtained using frequency bands with energy features on raw EEG data. EMD using all feature types on raw EEG data gave the most stable performance compared to all the methods, but with lower average validation accuracy than frequency bands. The performance of EMD was better using pre-processed EEG data when less than 60% of the dataset was tested but changed as the number of subjects increased. For the rest of the methods, better results were obtained with raw EEG data than pre-processed EEG data.

Results from using resting-state data from Dataset 2

The results obtained from resting-state data from Dataset 2 is presented in table 6.7 and plots of performance in fig. 6.7. DWT with mother wavelet Sym7 and statistical features, and PCA with 2 PCs applied on raw EEG data resulted in high validation accuracy as the number of subjects increased. When testing the full dataset (100%), the highest validation accuracy 0.97 was obtained using DWT, on both raw and pre-processed EEG data. DWT resulted in identical validation accuracy on all sizes

of the dataset when used on raw and pre-processed EEG data. EMD and frequency bands resulted in less stable and lower validation accuracy for this neuro-paradigm. For other methods than DWT, pre-processed EEG data resulted in lower validation accuracy compared to raw EEG data.

Data	**Method**	**Features**	**Number of subjects in percentage (Total: 26 subjects)**				
			20 %	**40 %**	**60 %**	**80 %**	**100 %**
Raw	EMD	Statistical	3-NN: 0.6400	linear SVM: 0.340	linear SVM: 0.363	linear SVM: 0.381	linear SVM: 0.339
	DWT	Bior 4.4 Statistical	RF-2: 0.720	RF-3: 0.540	RF-4: 0.388	RF-5: 0.438	RF-5: 0.400
	frequency bands	Energy, Fractal	linear SVM: 0.6400	RF-4: 0.520	RF-4: 0.563	RF-5: 0.419	RF-6: 0.415
	PCA	2 PC	RF-2: 0.800	linear SVM: 0.600	RF-4: 0.313	linear SVM: 0.314	linear SVM: 0.264
Pre-processed	EMD	Statistical	RF-5: 0.600	RF-5: 0.280	RF-3: 0.275	RF-2: 0.219	RF_3: 0.177
	DWT	Bior 4.4 Statistical	RF-2: 0.720	RF-5: 0.680	RF-4: 0.425	RF-5: 0.429	RF-5: 0.385
	frequency bands	Statistical	RF-5: 0.560	RF-2: 0.400	RF-4: 0.375	RF-5: 0.352	RF-6: 0.308
	PCA	2 PC	RF-2: 0.720	RF-3: 0.320	RF-5: 0.325	RF-3: 0.267	RF-4: 0.185

Table 6.5: Validation of ERP data from Dataset 1 using raw and processed EEG-signals containing five channels. Models were trained using session 1 and validated using session 2.

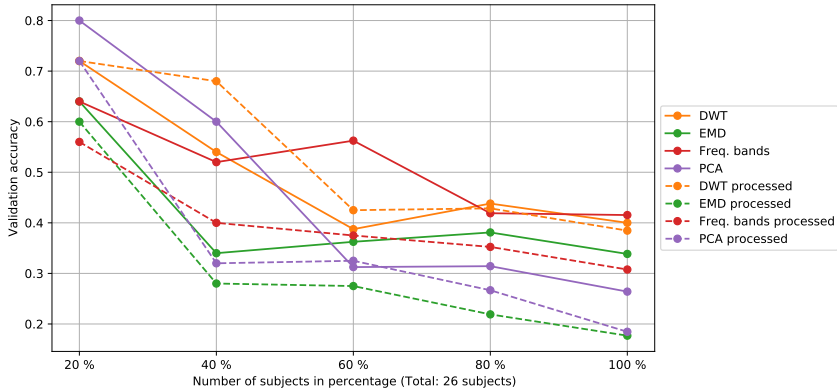

Figure 6.5: The evolution of validation accuracy of ERP data from Dataset 1 using raw and processed with EEG-signals containing five channels. Models were trained using session 1 and validated using session 2.

Data	Method	Features	Number of subjects in percentage (Total: 26 subjects)				
			20 %	**40 %**	**60 %**	**80 %**	**100 %**
Raw	EMD	Energy, Fractal, Statistical, HHT	RF-2: 0.520	RF-2: 0.380	RF-4: 0.450	RF-5: 0.419	RF-5: 0.369
	DWT	Sym 7, Statistical	RF-2: 0.520	2-NN: 0.580	RF-5: 0.425	RF-5: 0.457	RF-5: 0.423
	frequency bands	Energy, Fractal	RF-2: 0.680	RF-3: 0.600	RF-6: 0.613	linear SVM: 0.486	RF-5: 0.477
	PCA	2 PC	RF-2: 0.800	RF-5: 0.640	RF-5: 0.313	linear SVM: 0.305	linear SVM: 0.256
Pre-processed	EMD	Energy, Fractal	linear SVM: 0.560	RF-5: 0.500	RF-3: 0.488	RF-4: 0.371	RF-5: 0.285
	DWT	Bior 2.2 Energy	linear SVM: 0.640	linear SVM: 0.323	RF-5: 0.463	RF-5: 0.410	linear SVM: 0.640
	frequency bands	Energy, Fractal	linear SVM: 0.6400	RF-6: 0.362	RF-5: 0.575	RF-5: 0.429	RF-6: 0.362
	PCA	1 PC	2-NN: 0.560	RF-4: 0.320	RF-5: 0.413	RF-5: 0.305	RF-5: 0.262

Table 6.6: Validation of resting-state data from Dataset 1 using raw and processed EEG-signals containing five channels. Models were trained using session 1 and validated using session 2.

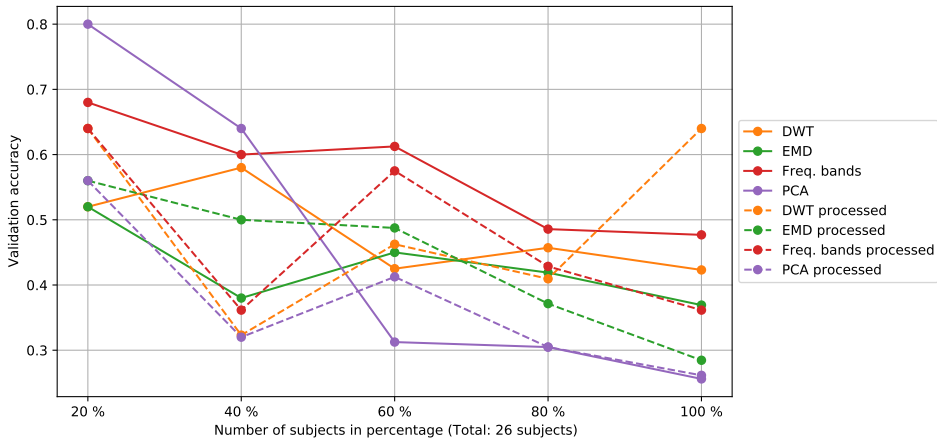

Figure 6.6: The evolution of validation accuracy of resting-state data from Dataset 1 using raw and processed with EEG-signals containing five channels. Models were trained using session 1 and validated using session 2.

Data	Method	Features	Number of subjects in percentage (Total: 40 subjects)				
			20 %	**40 %**	**60 %**	**80 %**	**100 %**
Raw	EMD	Energy, Fractal	RF-3: 0.550	RF-4: 0.675	RF-4: 0.458	RF-5: 0.419	RF-5: 0.360
	DWT	Sym7 Statistical	RF-2: 0.975	RF-3: 0.975	NB: 0.950	NB: 0.963	NB: 0.970
	frequency bands	Energy, Fractal	RF-4: 0.600	linear SVM: 0.663	RF-4 0.358	RF-5: 0.300	RF-5: 0.300
	PCA	2 PC	RF-2: 0.875	2-NN: 0.938	2-NN: 0.917	2-NN: 0.938	2-NN: 0.940
Pre-processed	EMD	Energy, hht, statistical	RF-3: 0.450	RF-5: 0.313	RF-4: 0.217	RF-5: 0.194	RF-5: 0.145
	DWT	Bior 4.4 Statistical	RF-2: 0.975	RF-3: 0.975	NB: 0.950	NB: 0.963	NB: 0.970
	frequency bands	Energy, Fractal	RF-4: 0.450	RF-5: 0.413	linear SVM: 0.458	linear SVM: 0.375	linear SVM: 0.355
	PCA	2 PC	RF-3: 0.500	RF-5: 0.338	linear SVM: 0.333	RF-5: 0.250	linear SVM: 0.250

Table 6.7: Validation of resting-state data from Dataset 2 using raw and processed EEG-signals containing five channels. Models were trained using session 1 and validated using session 2.

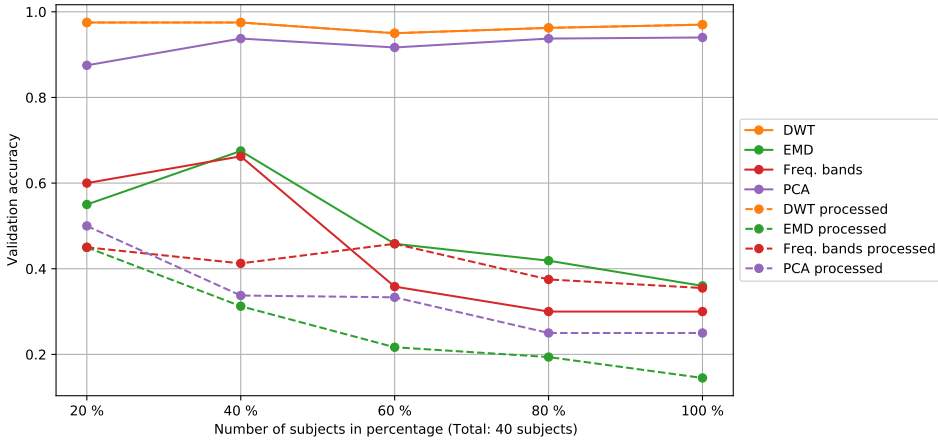

Figure 6.7: Validation of resting-state data from Dataset 2 using raw and processed EEG-signals containing five channels. Models were trained using session 1 and validated using session 2.

6.2 Offline classification using deep learning

DL classification was tested to classify subjects using time series sampled EEG voltage as input from different neuro-paradigms. Experiments are proposed as followed:

- Classification on raw EEG data using all channels from each dataset.
- Classification on raw EEG data using five channels from each dataset.

The experiments were conducted using EEGNet CNN as a classification model from [94] described in section 4.6.2. EEGNet architecture was used as it is designed explicitly for classifying raw EEG data with great performance.

The performance of the same classification model used on different neuro-paradigms was compared by using the same number of subjects and instances on each neuro-paradigm. Models were created and trained by utilizing 20 subjects from each dataset. The models were trained using session 1 with five instances per subject and validated using session 2 from each dataset. The training set was split into a training set and test set with a ratio of 0.33 to obtain training accuracy. The train-test-split function from Sckit-learn [93] was used to create the train and test set with a random seed set in Python to ensure reproducible results.

The models created for each neuro-paradigm are compared based on accuracy, loss, and the number of epochs (training rounds). Line plots were created to observe the model's ability to generalize and learning the problem. The line plots of the performance are called learning curves.

Classification accuracy alone hides the detail to understand the performance of the classification model better. Knowing what features were extracted from the raw data for classification when using CNN is not possible. Therefore, confusion matrices were created for each CNN model to see its choices for classification. A confusion matrix consists of a summary of prediction results on a classification problem. The confusion matrices present two dimensions: true label and predicted label. An identical set of classes, in this case, subjects, are presented in each dimension. The confusion matrix let us review if any specific subjects are more difficult to classify than others. Classification reports showing the precision, recall, and f1-scores are included in chapter B for each neuro-paradigm.

6.2.1 Deep learning classification using all channels

Each neuro-paradigm was tested using all channels to investigate the performance of CNN models using high-density EEG-recordings.

Results from using ERP data from Dataset 1

The model created using ERP data from Dataset 1 resulted in a model accuracy of 0.79 after 50 epochs. The learning curves in fig. 6.8 shows some generalization

obtained in the model as the validation loss decreased with the training loss. The confusion matrix for the created model in fig. 6.11 shows that five subjects were classified wrong.

Results from using resting-state data from Dataset 1

The model accuracy and validation loss using resting-state data from Dataset 1 are plotted in fig. 6.9. A model accuracy of 0.75 was obtained using 50 epochs. Both training loss and validation loss decreased as the number of epochs increased, which is an indication of learning. The confusion matrix for this model is visualized in fig. 6.12, showing that five subjects were classified wrong using this model.

Results from using resting-state data from Dataset 2

Model accuracy of 0.95 was obtained using resting-state data from Dataset 2 after 30 epochs. The learning curves in fig. 6.10 show that some generalization was obtained as the validation loss decreased with the training loss. The confusion matrix for this model presented in fig. 6.13 shows that all subjects except for one were classified correctly.

6.2.2 Deep learning classification with channel reduction

Each neuro-paradigm was tested using the same five channels presented in table 6.4 to investigate the performance of CNN models using low-density EEG-recordings.

Results from using ERP data from Dataset 1

ERP data from Dataset 1 resulted in a model accuracy of 0.37 after 100 epochs. The validation loss decreased with the number of epochs, and some learning was obtained, as shown in fig. 6.14. The confusion matrix presented in fig. 6.17 shows 12 subjects were classified wrong.

Results from using resting-state data from Dataset 1

Resting-state data from Dataset 1 resulted in a model accuracy of 0.53 after 50 epochs. The learning curves in fig. 6.15 indicate some learning in the model as the validation loss decreased with the training loss. The confusion matrix in fig. 6.18 shows that eight subjects were classified wrong with this model.

Results from using resting-state data from Dataset 2

The model using resting-state data from Dataset 2 resulted in a model accuracy of 0.75 after 50 epochs. The validation error decreased with the number of epochs increasing, with minor oscillations shown in fig. 6.16. Some learning was obtained in the model. The confusion matrix in fig. 6.19 shows that five subjects were classified wrong.

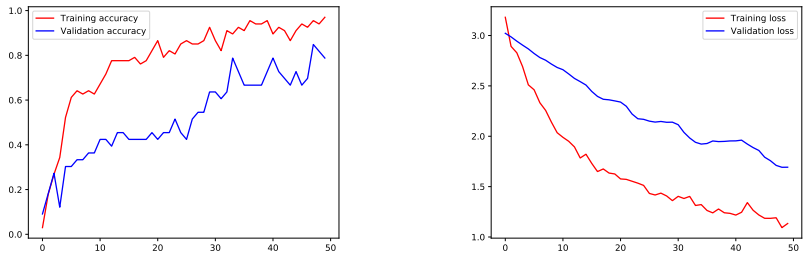

(a) Model accuracy **(b)** Model loss

Figure 6.8: Accuracy and loss values using ERP data from Dataset 1 with EEG-recording containing 56 channels.

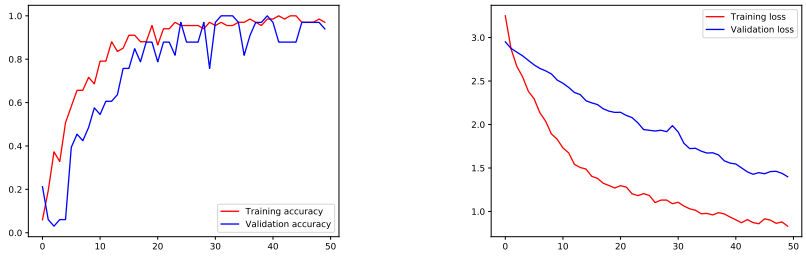

(a) Model accuracy **(b)** Model loss

Figure 6.9: Accuracy and loss values using resting-state data from Dataset 1 with EEG-recording containing 56 channels.

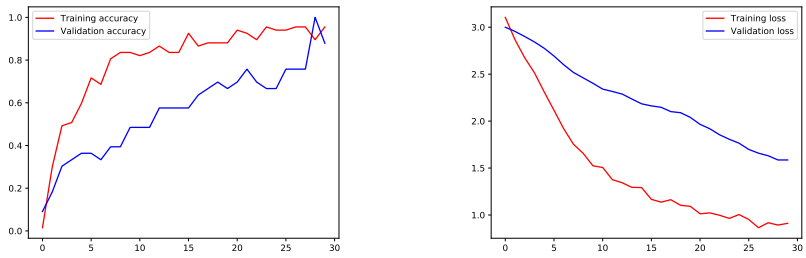

(a) Model accuracy **(b)** Model loss

Figure 6.10: Accuracy and loss values using resting-state data from Dataset 2 with EEG-recording containing 56 channels.

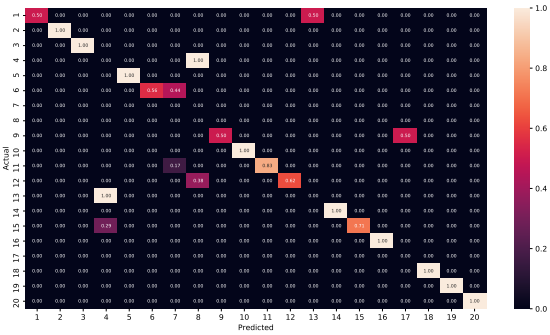

Figure 6.11: Confusion matrix of ERP data from Dataset 1 using 56 channels.

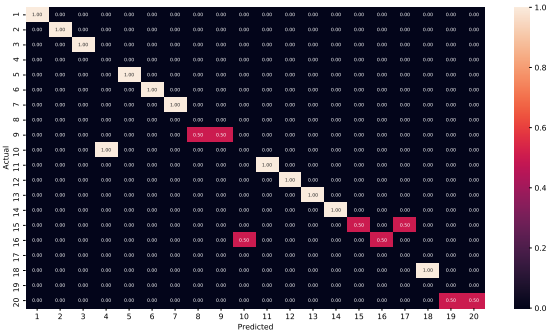

Figure 6.12: Confusion matrix of resting-state data from Dataset 1 using 56 channels.

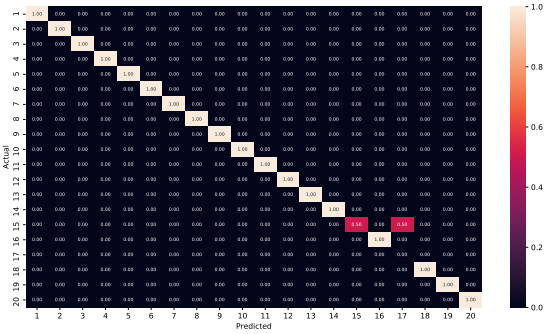

Figure 6.13: Confusion matrix of resting-state data from Dataset 2 using 68 channels.

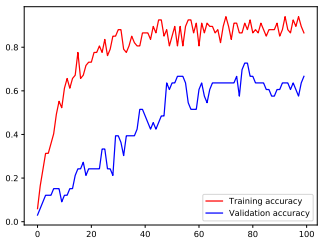

(a) Model accuracy

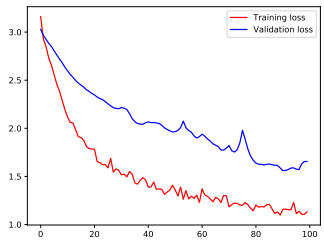

(b) Model loss

Figure 6.14: Accuracy and loss values using ERP data from Dataset 1 with EEG-recording containing five channels.

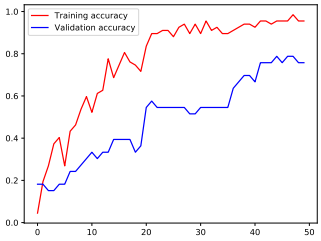

(a) Model accuracy

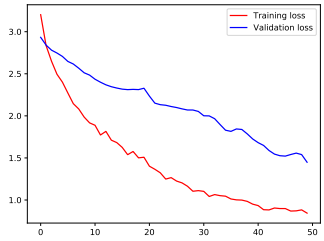

(b) Model loss

Figure 6.15: Accuracy and loss values using resting-state data from Dataset 1 with EEG-recording containing five channels.

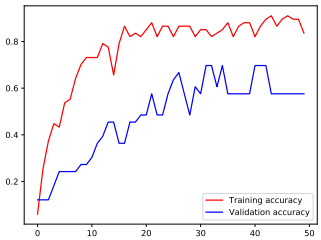

(a) Model accuracy

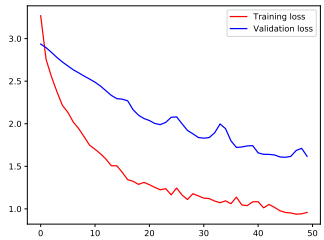

(b) Model loss

Figure 6.16: Accuracy and loss values using resting-state data from Dataset 2 with EEG-recording containing five channels.

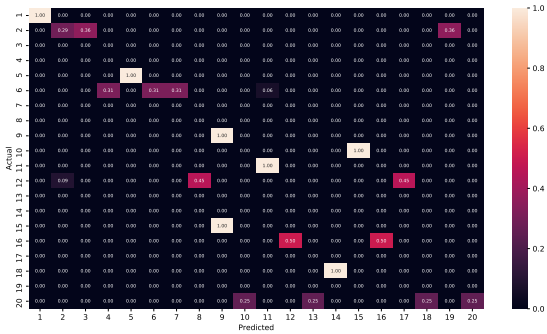

Figure 6.17: Confusion matrix of ERP data from Dataset 1 using five channels.

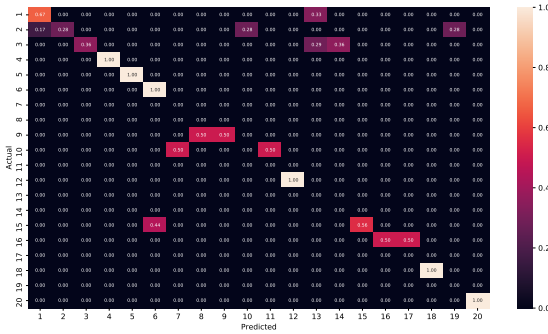

Figure 6.18: Confusion matrix of resting-state data from Dataset 1 using five channels.

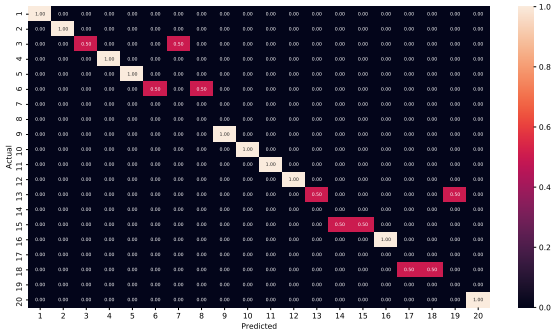

Figure 6.19: Confusion matrix of resting-state data from Dataset 2 using five channels.

6.3 Discussion of offline classification

6.3.1 Discussion - Machine learning

The combination of using frequency bands as a basis for extracting energy features and the RF classifier resulted in the highest validation accuracy for both ERP data and resting-state data from Dataset 1. This was the case when using all the channels in the dataset and channel reduction of raw EEG data. Furthermore, the same five channels were selected for ERP and resting-state data from Dataset 1. The dataset contains different neuro-paradigms (ERP and resting-state), and both were recorded executing the same experiment. This indicates that some similarity in brain activity was maintained through the whole experiment, even when the subjects were performing different brain tasks with different neuro-paradigms.

For resting-state data from Dataset 2, the combination of DWT with mother wavelet Sym7 as a basis for extracting energy features and k-NN as the classifier, resulted in the highest validation accuracy when using all channels from pre-processed EEG data. Using both raw and pre-processed EEG data with channel selection resulted in high validation accuracy using DWT with mother wavelet Sym7 as a basis for extracting statistical features and NB as the classifier.

Dataset 1 and Dataset 2 were collected from different experiments utilizing different protocols, and contain resting-state as a common neuro-paradigm. However, the best performance was achieved by using different methods, features, and classifiers for each dataset. The resting-states utilized from each experiment were acquired right after and before the subjects were engaging in another neuro-paradigm. The effect from the previous brain activity executed by the subjects may have continued while the subjects were at rest. This indicates that resting-state paradigms get affected by previous brain activity when creating a protocol with multiple neuro-paradigms. Therefore, the answer to the first research question is that a generalized ML model cannot be created when using resting-state as the common neuro-paradigm when extracted from different protocols.

Classifiers

Most of the validation accuracies were obtained using RF as a classifier. The RF was the dominant classifier when using ERP data fra Dataset 1 and produced half of the validation accuracies on resting-state data from Dataset 1 when using all the channels in the dataset. When using Dataset 1 and Dataset 2 with channel reduction, the RF classifier was dominant for all three neuro-paradigms. However, the overall highest validation accuracy between all three neuro-paradigm was obtained using k-NN as a classifier when using all the channels. When using channel reduction, the highest overall validation accuracy was obtained using NB. In both cases, the classifiers were applied to resting-state data from Dataset 2 containing 40 subjects. This indicates that k-NN and NB as robust classifiers when using high and low-density EEG-recording on numerous classes with few instances, respectively.

Pre-processing

For most of the methods, higher validation accuracies were obtained when no pre-processing was applied to the EEG-signals. Pre-processing used in this work may have removed the unique characteristics from the EEG-signals, making it more difficult to classify the signals. For instance, the EEG-signals in both datasets contained high-amplitude peaks in their high-frequency spectrum before any pre-processing was applied. After pre-processing, these peaks were removed as only low-frequency components were preserved, as shown in chapter A. These peaks could be essential for extracting unique features for classification.

For resting-state data from Dataset 2, the highest validation accuracy was obtained using DWT with pre-processed EEG data, with and without channel reduction. The pre-processing step applied to DWT was to remove the first coefficient containing high-frequency values. Some improvements can be seen in fig. 6.4, where the performance of DWT after pre-processing stays stable when testing on all sizes of the dataset, while DWT using raw EEG stabilizes as the number of subjects increases. In fig. 6.7, the performance of DWT resulted in identical accuracies with and without pre-processing. This indicated that using DWT on Dataset 2 manages to extract important features from the lower frequency domain since the removal of high-frequency components did not make any difference.

Channel Reduction

Classification with channel reduction resulted in lower accuracies as expected when compared to accuracies obtained using all the channels in the datasets. As the number of subjects increased, the validation accuracy stabilized for most of the methods. This shows that using a reduced number of channels can remove redundancy in data that may occur using large data from high-density EEG recordings.

High validation accuracies were obtained when using EEG-recordings containing five channels with DWT and PCA on resting-state data from Dataset 2. The highest validation accuracy of 0.97 was obtained using DWT on all subjects in the dataset. This shows the possibility of obtaining high accuracy with channel reduction, which is of interest when performing classification in real-time.

Choosing channels based on SD and MI gave channels containing relevant information on Dataset 2. However, this was not the case for Dataset 1 as the highest validation accuracy obtained with channel reduction was 0.64 with volatile performance. For ERP and resting-state data from Dataset 1, the same set of channels were selected. One reason for this is that both neuro-paradigms in Dataset 1 were recorded while conducting the same experiment, which resulted in the same channels becoming relevant for both neuro-paradigms. The use of channel selection methods should be considered in future work for finding channels with the highest importance for different neuro-paradigms. The use of the greedy algorithm used in [71] and NSGA purposed in [72] should be considered for channel selection.

Dimension Reduction

When applying dimension reduction on ERP and resting-state data from Dataset 1, PCA resulted in high accuracy when using a few subjects. As the number of subjects increased, accuracy and performance decreased. This was the case when using all the channels in the dataset and channel reduction. After pre-processing, Dataset 1 resulted in lower accuracy compared to raw EEG with dimension reduction. The classifiers manage to give high accuracy when using few PCs as features. However, no robust performance was achieved when adding more subjects to classify. Using more PCs as input to classifiers may create more stable performance, but also increase the computational complexity for training classification models.

Using PCA on resting-state data from Dataset 2, high accuracy and more stable performances were obtained, with and without channels reduction. The performance and accuracy when using PCA on raw EEG data from Dataset 2 is similar to DWT's performance on the same dataset. This shows that using a few PCs to represent the data can give similar performance as extracting features when using this resting-state as a neuro-paradigm. The accuracy and performance reduced when using PCA on pre-processed EEG data. The decreasing of PCA performance after pre-processing indicates that high-frequency components contain relevant information for creating PCs with maximum variance representing the EEG data.

6.3.2 Discussion - Deep learning

The accuracies obtained using CNN models for classification with no channel reduction was slightly better or similar to results obtained using ML with feature extraction. The CNN models managed to extract relevant features for automatic classification. Similar to ML, the highest accuracy using DL as a classification technique was obtained using the resting-state neuro-paradigm from Dataset 2.

When CNN models were created using a reduced number of channels, the accuracy decreased, and the number of epochs increased for both datasets. The accuracies obtained using CNN models were lower than accuracies obtained using the ML models with channel reduction. The increased number of epochs results in increased time for training models, which is not desired in real-time classification. Using a reduced number of channels for training CNN is important, as CNN already has high computational complexity to automatically extract relevant features for classification. Channel reduction can reduce the total complexity.

This answer the second research question of using DL as a classification technique when using a reduced number of channels. Using a reduced number of channels does not provide enough data for creating CNN models of high accuracy compared to using all channels in a dataset. The five channels chosen in this work may not be the most optimal channels for the datasets used in this work when using CNN. For future work, CNN should be tested using channel selection methods mentioned earlier.

6.3.3 Overall discussion of offline classification

A summary of the highest accuracies obtained from offline classification using ML and DL, on each neuro-paradigm, are presented in table 6.8 and table 6.9, respectively. The results presented are obtained using all subjects from each dataset. The overall highest accuracy of 1.00 was obtained using DWT with mother wavelet Sym7 as a basis for extracting energy features and a 2-NN classifier on pre-processed resting-state data from Dataset 2. This accuracy was achieved using all the channels in the dataset. Then second highest accuracy of 0.97 was obtained using the same resting-state data, with DWT using mother wavelet Sym7 as a basis for extracting statistical features and NB classifier. This was achieved using both pre-processed and raw EEG data with channel reduction. When using DL as a classification technique, resting-state data from Dataset 2 resulted in the highest accuracy of 0.95 using the CNN model without channel reduction after 30 epochs. These results indicate resting-state data from Dataset 2 as a desirable neuro-paradigm to using in real-time classification.

High accuracy was obtained using both classification techniques. However, when working in real-time, computational complexity and execution time are primary conditions to consider. For identification purposes, high accuracy values should be considered as well. DL classification gave high accuracy when all the channels in the datasets were utilized. ML gave high accuracy with and without channel reduction. Thus, the NB classifier with DWT using mother wavelet Sym7 as a basis for extracting statistical features is selected as a method for creating real-time classification. The system will be tested on pre-processed resting-state data from Dataset 2 with channel reduction. The real-time requirements are satisfied as the number of channels is reduced, the computational complexity of DWT is $\mathcal{O}(n \log_2 n)$, and NB's ability of fast computation when making predictions. Applying this method on pre-processed data will further decrease the computation as one less coefficient in DWT will be used for computing features.

Neuro-paradigm	Channels	Pre-processed	Method	Features	Classifier	Accuracy
Dataset 1:	56	No	frequency bands	Energy	RF	0.739
ERP	5	No	frequency bands	Energy	RF	0.415
Dataset 1:	56	No	frequency bands	Energy	RF	0.739
Resting-state	5	No	frequency bands	Energy	RF	0.477
Dataset 2:	68	Yes	DWT - Sym7	Energy	2-NN	0.995
Resting-state	**5**	**Yes**	**DWT - Sym7**	**Statistical**	**NB**	**0.970**

Table 6.8: Summary of the highest validation accuracies obtained offline using ML as a classification technique on each neuro-paradigms, using all channels and channel selection.

Neuro-paradigm	Channels	Epochs	Accuracy
Dataset 1: ERP	56	50	0.750
	5	100	0.370
Dataset 1 Resting-state	56	50	0.750
	5	50	0.530
Dataset 2: Resting-state	68	30	0.950
	5	50	0.750

Table 6.9: Summary of classifier accuracies obtained offline using DL as a classification technique on all three neuro-paradigms using all channels and channel selection.

6.4 Classification in real-time

A flowchart of the subject identification system created based on the results from offline-classification is illustrated in fig. 6.20.

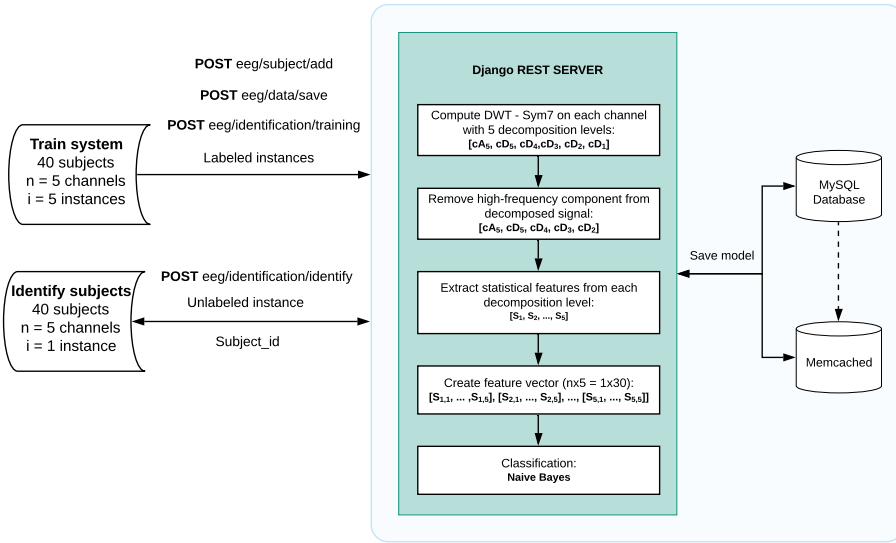

Figure 6.20: Flowchart of subject identification system used in real-time classification, with method chosen from offline classification.

The final system was created using ML with feature extraction. The system consists of DWT using mother wavelet Sym7 and five decomposition levels for decomposing EEG-signals into brain frequency bands. The high-frequency component is removed from the decomposed signal, and statistical features are extracted. The features extracted are then concatenated to a feature vector and is used as

input to the NB classifier for creating a classification model. The trained model is stored in the database for later use. Two experiments are purposed for real-time classification:

1. Train the system using session 1 and predict subjects using sessions 2, 3, 4, and 5.
2. Train the system using session 5 and predict subjects using sessions 1, 2, 3, and 4.

These experiments aim at assessing the performance of the EEG-based subject identification system for individual identification with respect to subjects, on systems trained on different sessions from the same dataset.

The system performance is evaluated based on the TAR of subjects on each experiment.

$$TAR = \frac{\text{the total number of subjects correctly detected}}{\text{the total number of subjects}}$$

The resting-state data from Dataset 2, acquired from a Spatial Attention experiment, was chosen as a neuro-paradigm for this system. All 40 subjects from Dataset 2 were used to test the system's performance and to observe the robustness of the selected method. To resemble a real-world application, five instances per subject were used to train the models and one instance for predicting the subject. Using a few instances for both training and predicting reduces the computation time and increases usability when comparing to real-life applications. One epoch of 2 *sec.* was created from each instance. The models were therefore trained on 10 *sec.* of EEG recordings, and predicted on 2 *sec.* from each subject.

System trained on session 1 from Dataset 2

The results obtained using session 1 for training the system are presented in fig. 6.21. When the subject capacity was less than six, the TAR reached 1.00 for all the sessions tested. The TAR continued to stay at 1.00 until 12 subjects were added to the system with session 3. Lowest TAR was obtained using session 5 to identify the subjects and stabilized around 0.75 when the subject capacity was from 31-39. The highest TAR was obtained using session 3 with stable TAR around 0.95 when the subject capacity was from 13-32. When all 40 subjects were added to the system, the highest TAR obtained was 0.93.

System trained on session 5 from Dataset 2

The results obtained using session 5 for training the system are presented in fig. 6.22. When the subject capacity was less than seven, the TAR reached 1.00 for all the sessions tested. The TAR rapidly decreased when more than eight subjects were added to the system and then stabilized as the number of subjects increased. The best performance was obtained when using session 4, which resulted in a TAR

of 0.63 when all subjects were added. Sessions 1, 2, and 3 resulted in lower TAR after seven subjects were added to the system with no improvements when the subject capacity increased.

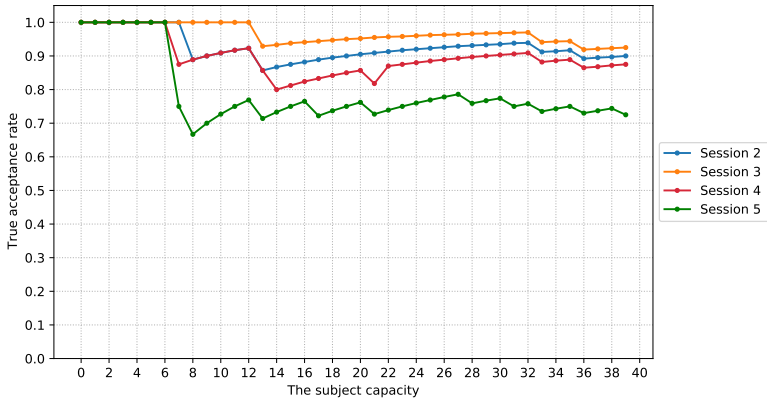

Figure 6.21: TAR in the capacity dimension. Models were trained using session 1 from Dataset 2 and tested using session 2, 3, 4 and 5.

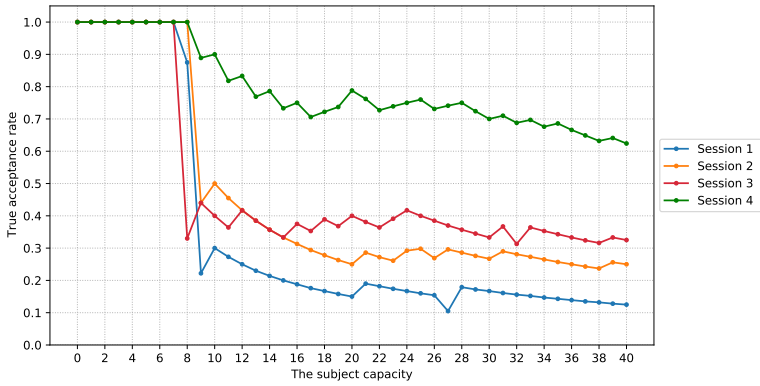

Figure 6.22: TAR int the capacity dimension. Models trained using session 5 from Dataset 2 and tested using session 1, 2, 3 and 4.

6.5 Discussion of real-time classification

Identical systems were used for identifying subjects in both experiments; however, high TAR was obtained in the first experiment and lower TAR in the second experiment. The only difference between the two experiments when creating the system was the session used for training the classification models. The TARs obtained from both experiments indicate that a better-trained model was used to identify subjects in the first experiment than in the second experiment. This shows the importance of what data is used for training a model, which can affect the end result. In this dataset, session 1 contains a better collection of EEG signals as a better-trained model was obtain using this session.

In the second experiment, TAR started to decrease after subject nr.9 was added to the system. This was a trend in all the sessions used for testing. The reason for this could be that subject nr.9 did not follow the given neuro-paradigm while recording the EEG-signals, resulting in unique EEG-signals for subjects nr.9 compared to other subjects. The features extracted for subject nr.9 may have changed the trained NB model to dominate other subjects' prediction as subject nr.9.

Another reason for the low TAR obtained in the second experiment could be the reduced number of channels used for identification. Using all the channels in the dataset for training the models could result in higher model accuracy, which will result in higher TAR. Increasing the number of channels will increase the computation time, creating a trade-off between the number of channels used for identification and the computation complexity.

High TAR was obtained when testing all four sessions in the first experiment. In the best case, a TAR of 0.93 was obtained when all 40 subjects were added. A real-time subject identification experiment from state-of-the-art work [76], resulted in stable TAR at 0.70 when testing on a subject capacity of 12-20. Compared to that experiment, better performance was achieved in this present work. This supports the selected method from offline-classification used for creating the final identification system.

The created subject identification system managed to obtain high TAR when using 40 subjects, using one instance per subject when predicting. This indicates a robust response to the feature extraction method selected and works well for the selected neuro-paradigm. The time used for training a model when 40 subjects were added to the system was 0.18 *sec.*, and 0.07 *sec.* for identifying one subject.

Chapter 7

Conclusion

Two types of neuro-paradigms were used in this work when testing ML and DL as classification techniques. High accuracy was obtained when using resting-state neuro-paradigm acquired from a spatial attention experiment on both classification techniques.

Different pre-processing techniques were applied to EEG-signals for improving the SNR. When using DWT as a signal decomposition method, the first coefficient was removed to increase the SNR, which resulted in higher accuracy. Applying band-pass filters of $1.0 - 20.0$ Hz and $0.5 - 40.0$ Hz when using EMD, frequency bands, and PCA resulted in lower accuracy. The methods used alone resulted in higher accuracy.

Channel reduction based on SD and MI was utilized on different classification techniques to reduce the computation complexity in real-time classification. The selected channels resulted in high accuracy for the resting-state neuro-paradigm acquired from the spatial attention experiment when used with DWT. For all other methods and neuro-paradigms, the selected channels resulted in low accuracy. Channel reduction based on SD and MI was not optimal for selecting a reduced number of relevant channels for the given neuro-paradigms.

The use of PCA as a method for dimension reduction was studied. A maximum of 2 PCs was used for classification, which resulted in high accuracy when using a few number of subjects. The accuracy and performance decreased as the number of subjects increased. Applying PCA on pre-processing EEG-signals resulted in lower accuracy. This method can be applied for identification systems containing a low number of subjects using raw EEG-signals.

High accuracy was obtained when using ML as a classification technique when using all channels and channels reduction. Similar results were obtained using DL as a classification when all channels were utilized. When using low-density EEG-recording, DL resulted in lower accuracy than using ML. The use of low-density

EEG-recording does not provide enough data for DL classification, making ML classification more desirable for real-time classification.

The feature-based ML classification was chosen to create a subject identification system as it was optimal for real-time classification. The system was created using DWT with mother wavelet Sym7 and NB as classifier on pre-processed EEG data with channel reduction. The resting-state neuro-paradigm from spatial attention experiment was chosen as EEG data to train the system and identify the subjects. The highest TAR of 0.93 was obtained with 40 subjects added to the system. Based on the results, it can be concluded that the selected method is suitable for creating an EEG-based subject identification system.

7.1 Future work

To apply a EEG-based biometric system in real-life applications, many factors need to be satisfied. The number of electrodes used for data collection has a significant impact on the system's usability: a large number of electrodes may increase the difficulty of deploying the system in real-life scenarios. The length of the EEG recordings employed for system training and processing time are important factors. Lastly, the training and testing duration in seconds, the time spent by users, and the computational efficiency matters.

The subject identification system created in this work fulfills these conditions as high TAR was obtained with 40 subjects using a few instances for training and identification, with only five channels from each EEG recording. However, this was achieved using pre-collected EEG data on a simulated system. Future work should, therefore, recreate the protocol used in this work and the methods chosen while recording EEG-signals in real-time to investigate the performance in real-life applications.

The brain activity conducted by a subject, and the number of electrodes used for acquiring EEG signals impact the real-time classification of subjects. Low-cost sensor headsets are, therefore, of interest. In future work, various channel selection methods should be tested to find the optimal number of electrodes to use for the given protocol. Only the chosen electrodes should then be used for recording EEG signals in real-time. Pre-processing methods suitable for real-time application should also be applied for improving the SNR when aquiring EEG-signals.

The selected system should be tested on a more extensive number of subjects (more than 100) to confirm the selection of methods and the choice of dataset. The system should also be tested on EGG data collected over more extended periods of time to assess their aging performance.

Bibliography

[1] Simon Singh. *The code book: the science of secrecy from ancient Egypt to quantum cryptography*. Anchor, 2000.

[2] Hugh Sebag-Montefiore. *Enigma: the battle for the code*. Weidenfeld & Nicolson, 2011.

[3] Simon Fenn. A brief history of security. `https://www.vodafone.com/business/news-and-insights/blog/gigabit-thinking/a-brief-history-of-security`. Last accessed 21 May 2020.

[4] Anil K Jain, Arun Ross, and Salil Prabhakar. An introduction to biometric recognition. *IEEE Transactions on circuits and systems for video technology*, 14(1):4–20, 2004.

[5] Anil K Jain, Ruud Bolle, and Sharath Pankanti. *Biometrics: personal identification in networked society*, volume 479. Springer Science & Business Media, 2006.

[6] T Sabhanayagam, V Prasanna Venkatesan, and K Senthamaraikannan. A comprehensive survey on various biometric systems. *International Journal of Applied Engineering Research*, 13(5):2276–2297, 2018.

[7] Qiong Gui, Maria Blondet, Sarah Laszlo, and Zhanpeng Jin. A survey on brain biometrics. *ACM Computing Surveys*, 51:1–38, 02 2019.

[8] CEM Van Beijsterveldt and DI Boomsma. Genetics of the human electroencephalogram (eeg) and event-related brain potentials (erps): a review. *Human genetics*, 94(4):319–330, 1994.

[9] Eelco FM Wijdicks, Panayiotis N Varelas, Gary S Gronseth, and David M Greer. Evidence-based guideline update: determining brain death in adults: report of the quality standards subcommittee of the american academy of neurology. *Neurology*, 74(23):1911–1918, 2010.

[10] Luis Moctezuma and Marta Molinas. Sex differences observed in a study of eeg of linguistic activity and resting-state: Exploring optimal eeg channel configurations. 02 2019.

[11] P. Campisi and D. L. Rocca. Brain waves for automatic biometric-based user recognition. *IEEE Transactions on Information Forensics and Security*, 9(5):782–800, 2014.

[12] Julie Haga. Biometric system using eeg signals from resting-state and one-class classifiers. Master's thesis, NTNU, 2020.

[13] Shobiha K. Premkumar. Eeg-based biometric system for subject identification using empirical mode decomposition and frequency bands. unpublished, 2019.

[14] Jonathan Wolpaw and Elizabeth Winter Wolpaw. *Brain-computer interfaces: principles and practice*. OUP USA, 2012.

[15] D Puthankattil Subha, Paul K Joseph, Rajendra Acharya, and Choo Min Lim. Eeg signal analysis: a survey. *Journal of medical systems*, 34(2):195–212, 2010.

[16] Jeffrey W Britton, Lauren C Frey, Jennifer L Hopp, Pearce Korb, MZ Koubeissi, WE Lievens, Elia M Pestana-Knight, and EK Louis St. Electroencephalography (eeg): An introductory text and atlas of normal and abnormal findings in adults, children, and infants. 2016.

[17] David Steyrl, Reinmar J Kobler, Gernot R Müller-Putz, et al. On similarities and differences of invasive and non-invasive electrical brain signals in brain-computer interfacing. *Journal of Biomedical Science and Engineering*, 9(08):393, 2016.

[18] Luis Fernando Nicolas-Alonso and Jaime Gomez-Gil. Brain computer interfaces, a review. *Sensors*, 12(2):1211–1279, 2012.

[19] George H Klem, Hans Otto Lüders, HH Jasper, C Elger, et al. The ten-twenty electrode system of the international federation. *Electroencephalogr Clin Neurophysiol*, 52(3):3–6, 1999.

[20] Larry Squire, Darwin Berg, Floyd E Bloom, Sascha Du Lac, Anirvan Ghosh, and Nicholas C Spitzer. *Fundamental neuroscience*. Academic Press, 2012.

[21] Paul L Nunez, Ramesh Srinivasan, et al. *Electric fields of the brain: the neurophysics of EEG*. Oxford University Press, USA, 2006.

[22] Patrizio Campisi and Daria La Rocca. Brain waves for automatic biometric-based user recognition. *IEEE transactions on information forensics and security*, 9(5):782–800, 2014.

[23] J Craig Henry. Electroencephalography: Basic principles, clinical applications, and related fields. *Neurology*, 67(11):2092–2092, 2006.

[24] Shravani Sur and VK Sinha. Event-related potential: An overview. *Industrial psychiatry journal*, 18(1):70, 2009.

[25] Ali Haider and Reza Fazel-Rezai. Application of p300 event-related potential in brain-computer interface. *Event-related Potentials and Evoked Potentials. INTECH*, pages 19–38, 2017.

[26] Yijun Wang, Ruiping Wang, Xiaorong Gao, Bo Hong, and Shangkai Gao. A practical vep-based brain-computer interface. *IEEE Transactions on Neural Systems and Rehabilitation Engineering*, 14(2):234–240, 2006.

[27] Marcos Del Pozo-Banos, Jesús B Alonso, Jaime R Ticay-Rivas, and Carlos M Travieso. Electroencephalogram subject identification: A review. *Expert Systems with Applications*, 41(15):6537–6554, 2014.

[28] Anil K Jain, Arun Ross, and Salil Prabhakar. An introduction to biometric recognition. *IEEE Transactions on circuits and systems for video technology*, 14(1):4–20, 2004.

[29] James Wayman, Rene McIver, Peter Waggett, Stephen Clarke, Masanori Mizoguchi, Christoph Busch, Nicolas Delvaux, and Andrey Zudenkov. Vocabulary harmonisation for biometrics: the development of iso/iec 2382 part 37. *IET biometrics*, 3(1):1–8, 2013.

[30] James L Wayman. Fundamentals of biometric authentication technologies. *International Journal of Image and Graphics*, 1(01):93–113, 2001.

[31] Emanuele Maiorana, Daria La Rocca, and Patrizio Campisi. Eigenbrains and eigentensorbrains: Parsimonious bases for eeg biometrics. *Neurocomputing*, 171:638–648, 2016.

[32] Lei Yu and Huan Liu. Feature selection for high-dimensional data: A fast correlation-based filter solution. In *Proceedings of the 20th international conference on machine learning (ICML-03)*, pages 856–863, 2003.

[33] Md Kafiul Islam, Amir Rastegarnia, and Zhi Yang. Methods for artifact detection and removal from scalp eeg: A review. *Neurophysiologie Clinique/Clinical Neurophysiology*, 46(4-5):287–305, 2016.

[34] Dimitris G Manolakis and Vinay K Ingle. *Applied digital signal processing: theory and practice*. Cambridge University Press, 2011.

[35] Rogelio Ramos, Benjamin Valdez-Salas, Roumen Zlatev, Michael Schorr Wiener, and Jose María Bastidas Rull. The discrete wavelet transform and its application for noise removal in localized corrosion measurements. *International Journal of Corrosion*, 2017, 2017.

[36] D Puthankattil Subha, Paul K Joseph, Rajendra Acharya, and Choo Min Lim. Eeg signal analysis: a survey. *Journal of medical systems*, 34(2):195–212, 2010.

[37] Maja Bitenc, DS Kieffer, and K Khoshelham. Evaluation of wavelet denoising methods for small-scale joint roughness estimation using terrestrial laser scanning. *ISPRS Annals of Photogrammetry, Remote Sensing & Spatial Information Sciences*, 2, 2015.

[38] A.E. Hassanien, M.F. Tolba, M. Elhoseny, and M. Mostafa. *The International Conference on Advanced Machine Learning Technologies and Applications (AMLTA2018)*. Advances in Intelligent Systems and Computing. Springer International Publishing, 2018.

[39] Hasan Ocak. Automatic detection of epileptic seizures in eeg using discrete wavelet transform and approximate entropy. *Expert Systems with Applications*, 36(2):2027–2036, 2009.

[40] Na Ji, Liang Ma, Hui Dong, and Xuejun Zhang. Eeg signals feature extraction based on dwt and emd combined with approximate entropy. *Brain sciences*, 9(8):201, 2019.

[41] Md Khademul Islam Molla, Md Rabiul Islam, Toshihisa Tanaka, and Tomasz M Rutkowski. Artifact suppression from eeg signals using data adaptive time domain filtering. *Neurocomputing*, 97:297–308, 2012.

[42] Norden E Huang, Zheng Shen, Steven R Long, Manli C Wu, Hsing H Shih, Quanan Zheng, Nai-Chyuan Yen, Chi Chao Tung, and Henry H Liu. The empirical mode decomposition and the hilbert spectrum for nonlinear and non-stationary time series analysis. *Proceedings of the Royal Society of London. Series A: mathematical, physical and engineering sciences*, 454(1971):903–995, 1998.

[43] Norden Eh Huang. *Hilbert-Huang transform and its applications*, volume 16. World Scientific, 2014.

[44] Yunchao Gao, Guangtao Ge, Zhengyan Sheng, and Enfang Sang. Analysis and solution to the mode mixing phenomenon in emd. In *2008 Congress on Image and Signal Processing*, volume 5, pages 223–227. IEEE, 2008.

[45] Zhaohua Wu and Norden E Huang. Ensemble empirical mode decomposition: a noise-assisted data analysis method. *Advances in adaptive data analysis*, 1(01):1–41, 2009.

[46] Pier Paolo Ippolito. Feature extraction techniques, Oct 2019. Last accessed 13 April 2020.

[47] Girish Chandrashekar and Ferat Sahin. A survey on feature selection methods. *Computers & Electrical Engineering*, 40(1):16–28, 2014.

[48] John M O'Toole, Andriy Temko, and Nathan Stevenson. Assessing instantaneous energy in the eeg: a non-negative, frequency-weighted energy operator. In *2014 36th Annual International Conference of the IEEE Engineering in Medicine and Biology Society*, pages 3288–3291. IEEE, 2014.

[49] Francesca Finotello, Fabio Scarpa, and Mattia Zanon. Eeg signal features extraction based on fractal dimension. In *2015 37th Annual International Conference of the IEEE Engineering in Medicine and Biology Society (EMBC)*, pages 4154–4157. IEEE, 2015.

[50] Cindy Goh, Brahim Hamadicharef, Goeff Henderson, and Emmanuel Ifeachor. Comparison of fractal dimension algorithms for the computation of eeg biomarkers for dementia. 2005.

[51] Christian Flores Vega and Julien Noel. Parameters analyzed of higuchi's fractal dimension for eeg brain signals. In *2015 Signal Processing Symposium (SPSympo)*, pages 1–5. IEEE, 2015.

[52] Tomoyuki Higuchi. Approach to an irregular time series on the basis of the fractal theory. *Physica D: Nonlinear Phenomena*, 31(2):277–283, 1988.

[53] Su Yang and Farzin Deravi. Novel hht-based features for biometric identification using eeg signals. In *2014 22nd International Conference on Pattern Recognition*, pages 1922–1927. IEEE, 2014.

[54] Ian T Jolliffe and Jorge Cadima. Principal component analysis: a review and recent developments. *Philosophical Transactions of the Royal Society A: Mathematical, Physical and Engineering Sciences*, 374(2065):20150202, 2016.

[55] T Kourti. Multivariate statistical process control and process control, using latent variables. 2009.

[56] Nils J Nilsson. Stuart russell and peter norvig, artificial intelligence: A modern approach. *Artificial intelligence*, 82(1-2):369–380, 1996.

[57] Jason Brownlee. Develop k-nearest neighbors in python from scratch, Feb 2020. Last accessed 24 April 2020.

[58] 1.6. Nearest Neighbors. `https://scikit-learn.org/stable/modules/neighbors.html`, 2019. Last accessed 24 April 2020.

[59] J. Ross Quinlan. Induction of decision trees. *Machine learning*, 1(1):81–106, 1986.

[60] Jiawei Han, Jian Pei, and Micheline Kamber. *Data mining: concepts and techniques*. Elsevier, 2011.

[61] 1.10. Decision Trees. `https://scikit-learn.org/stable/modules/tree.html`, 2019. Last accessed 24 April 2020.

[62] Andy Liaw, Matthew Wiener, et al. Classification and regression by randomforest. *R news*, 2(3):18–22, 2002.

[63] Jason Brownlee. How to develop a naive bayes classifier from scratch in python, Jan 2020. Last accessed 24 April 2020.

[64] Mia K. Stern, Joseph E. Beck, and Beverly Park Woolf. Naïve bayes classifiers for user modeling. In *Proceedings of the Conference on User Modeling*, 1999.

[65] Alexander Craik, Yongtian He, and Jose L Contreras-Vidal. Deep learning for electroencephalogram (eeg) classification tasks: a review. *Journal of neural engineering*, 16(3):031001, 2019.

[66] Bernard Marr. What is deep learning ai? a simple guide with 8 practical examples. Last accessed 28 March 2020.

[67] Yann LeCun, Yoshua Bengio, and Geoffrey Hinton. Deep learning. *nature*, 521(7553):436–444, 2015.

[68] Shuo Feng, Huiyu Zhou, and Hongbiao Dong. Using deep neural network with small dataset to predict material defects. *Materials & Design*, 162:300–310, 2019.

[69] Luis Alfredo Moctezuma and Marta Molinas. Eeg-based subjects identification based on biometrics of imagined speech using emd. In *International Conference on Brain Informatics*, pages 458–467. Springer, 2018.

[70] Luis Alfredo Moctezuma and Marta Molinas. Event-related potential from eeg for a two-step identity authentication system. In *2019 IEEE 17th International Conference on Industrial Informatics (INDIN)*, volume 1, pages 392–399. IEEE, 2019.

[71] Luis Alfredo Moctezuma and Marta Molinas. Subject identification from low-density eeg-recordings of resting-states: A study of feature extraction and classification. In *Future of Information and Communication Conference*, pages 830–846. Springer, 2019.

[72] Luis Alfredo Moctezuma and Marta Molinas. Multi-objective optimization for eeg channel selection and accurate intruder detection in an eeg-based subject identification system. *Scientific Reports*, 10(1):1–12, 2020.

[73] Su Yang and Farzin Deravi. Novel hht-based features for biometric identification using eeg signals. In *2014 22nd International Conference on Pattern Recognition*, pages 1922–1927. IEEE, 2014.

[74] Ramaswamy Palaniappan. Method of identifying individuals using vep signals and neural network. *IEE Proceedings-Science, Measurement and Technology*, 151(1):16–20, 2004.

[75] Luis Alfredo Moctezuma and Maria Marta Molinas Cabrera. Towards an api for eeg-based imagined speech classification. In *ITISE 2018-International Conference on Time Series and Forecasting*, 2018.

[76] Bin Hu, Quanying Liu, Qinglin Zhao, Yanbing Qi, and Hong Peng. A real-time electroencephalogram (eeg) based individual identification interface for mobile security in ubiquitous environment. In *2011 IEEE Asia-Pacific Services Computing Conference*, pages 436–441. IEEE, 2011.

[77] Bo Hjorth. Eeg analysis based on time domain properties. *Electroencephalography and clinical neurophysiology*, 29(3):306–310, 1970.

[78] P. Campisi and D. L. Rocca. Brain waves for automatic biometric-based user recognition. *IEEE Transactions on Information Forensics and Security*, 9(5):782–800, 2014.

[79] Abdulhamit Subasi and M Ismail Gursoy. Eeg signal classification using pca, ica, lda and support vector machines. *Expert systems with applications*, 37(12):8659–8666, 2010.

[80] Ramaswamy Palaniappan, S Anandan, and Paramesran Raveendran. Two level pca to reduce noise and eeg from evoked potential signals. In *7th International Conference on Control, Automation, Robotics and Vision, 2002. ICARCV 2002.*, volume 3, pages 1688–1693. IEEE, 2002.

[81] Ramaswamy Palaniappan and Danilo P Mandic. Energy of brain potentials evoked during visual stimulus: A new biometric? In *International Conference on Artificial Neural Networks*, pages 735–740. Springer, 2005.

[82] Lan Ma, James W Minett, Thierry Blu, and William SY Wang. Resting state eeg-based biometrics for individual identification using convolutional neural networks. In *2015 37th Annual International Conference of the IEEE Engineering in Medicine and Biology Society (EMBC)*, pages 2848–2851. IEEE, 2015.

[83] Hubert Cecotti and Axel Graser. Convolutional neural networks for p300 detection with application to brain-computer interfaces. *IEEE transactions on pattern analysis and machine intelligence*, 33(3):433–445, 2010.

[84] Perrin Margaux, Maby Emmanuel, Daligault Sébastien, Bertrand Olivier, and Mattout Jérémie. Objective and subjective evaluation of online error correction during p300-based spelling. *Advances in Human-Computer Interaction*, 2012, 2012.

[85] Hiroshi Morioka, Atsunori Kanemura, Satoshi Morimoto, Taku Yoshioka, Shigeyuki Oba, Motoaki Kawanabe, and Shin Ishii. Decoding spatial attention by using cortical currents estimated from electroencephalography with near-infrared spectroscopy prior information. *Neuroimage*, 90:128–139, 2014.

[86] Hiroshi Morioka, Atsunori Kanemura, Jun-ichiro Hirayama, Manabu Shikauchi, Takeshi Ogawa, Shigeyuki Ikeda, Motoaki Kawanabe, and Shin Ishii. Learning a common dictionary for subject-transfer decoding with resting calibration. *NeuroImage*, 111:167–178, 2015.

[87] Robert S Fisher, WR Webber, Ronald P Lesser, Santiago Arroyo, and Sumio Uematsu. High-frequency eeg activity at the start of seizures. *Journal of clinical neurophysiology: official publication of the American Electroencephalographic Society*, 9(3):441–448, 1992.

[88] Daoud Boutana, Messaoud Benidir, and Braham Barkat. On the selection of intrinsic mode function in emd method: application on heart sound signal. In *2010 3rd International Symposium on Applied Sciences in Biomedical and Communication Technologies (ISABEL 2010)*, pages 1–5. IEEE, 2010.

[89] Julie Haga. Eeg-based biometric system using discrete wavelet transform and principal component analysis. unpublished, 2019.

[90] Dawid Laszuk. Python implementation of empirical mode decomposition algorithm. `http://www.laszukdawid.com/codes`, 2017.

[91] Gregory R. Lee, Ralf Gommers, Filip Wasilewski, Kai Wohlfahrt, and Aaron O'Leary. Pywavelets: A python package for wavelet analysis. volume 4(36), page 1237, 2019.

[92] Pauli Virtanen, Ralf Gommers, Travis E. Oliphant, Matt Haberland, Tyler Reddy, David Cournapeau, Evgeni Burovski, Pearu Peterson, Warren Weckesser, Jonathan Bright, Stéfan J. van der Walt, Matthew Brett, Joshua Wilson, K. Jarrod Millman, Nikolay Mayorov, Andrew R. J. Nelson, Eric Jones, Robert Kern, Eric Larson, CJ Carey, İlhan Polat, Yu Feng, Eric W. Moore, Jake Vand erPlas, Denis Laxalde, Josef Perktold, Robert Cimrman, Ian Henriksen, E. A. Quintero, Charles R Harris, Anne M. Archibald, Antônio H. Ribeiro, Fabian Pedregosa, Paul van Mulbregt, and SciPy 1. 0 Contributors. SciPy 1.0: Fundamental Algorithms for Scientific Computing in Python. *Nature Methods*, 17:261–272, 2020.

[93] F. Pedregosa, G. Varoquaux, A. Gramfort, V. Michel, B. Thirion, O. Grisel, M. Blondel, P. Prettenhofer, R. Weiss, V. Dubourg, J. Vanderplas, A. Passos, D. Cournapeau, M. Brucher, M. Perrot, and E. Duchesnay. Scikit-learn: Machine learning in Python. *Journal of Machine Learning Research*, 12:2825–2830, 2011.

[94] Vernon J Lawhern, Amelia J Solon, Nicholas R Waytowich, Stephen M Gordon, Chou P Hung, and Brent J Lance. Eegnet: a compact convolutional neural network for eeg-based brain–computer interfaces. *Journal of neural engineering*, 15(5):056013, 2018.

[95] Abhijit Bhattacharyya and Ram Bilas Pachori. A multivariate approach for patient-specific eeg seizure detection using empirical wavelet transform. *IEEE Transactions on Biomedical Engineering*, 64(9):2003–2015, 2017.

[96] Django (version 1.5). `https://djangoproject.com`, 2013.

Appendix A

Pre-processing

The frequency spectrum of pre-processed ERP data and resting-state data from Dataset 1 and resting-state Dataset 2 are presented in fig. A.2, fig. A.3 and fig. A.2, respectively. After pre-processing, the powerline noises in all the neuro-paradigms are suppressed as they exist in the high-frequency domain of the frequency spectrum $>$ 50 Hz. The high-amplitude components at 0 Hz, causing offset in the signals, are also suppressed after filtering the signals.

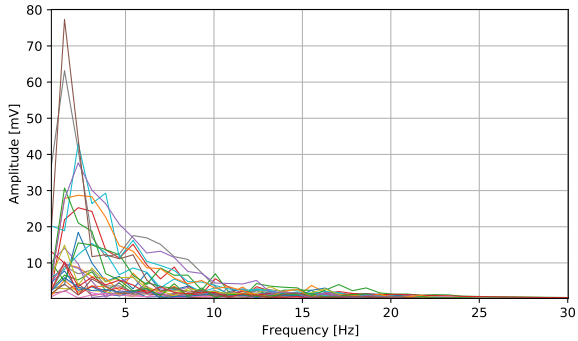

Figure A.1: Frequency spectrum of pre-processed ERP data from Dataset 1.

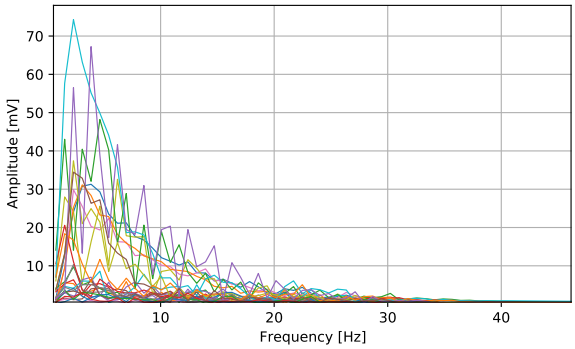

Figure A.2: Frequency spectrum of pre-processed resting-state data from Dataset 1.

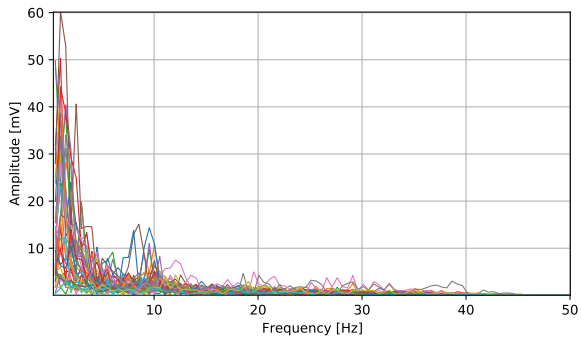

Figure A.3: Frequency spectrum of pre-processed resting-state data from Dataset 2.

Appendix B

CNN Classification reports

The classification report for the CNN models created in section 6.2 are included in the following chapter. The reports are presented for each neuro-paradigm when testing on both high and low-density EEG recordings.

Class	Precision		Recall		f1-score		support	
	Ch. 56	**Ch. 5**	**Ch. 56**	**Ch. 5**	**Ch. 56**	**Ch. 5**	**Ch. 56**	**Ch. 5**
1	0.50	1.00	1.00	1.00	0.67	1.00	5	5
2	1.00	0.29	1.00	0.80	1.00	0.42	5	5
3	1.00	0.00	1.00	0.00	1.00	0.00	5	5
4	0.00	0.00	0.00	0.00	0.00	0.00	5	5
5	1.00	1.00	1.00	1.00	1.00	1.00	5	5
6	0.56	0.31	1.00	1.00	0.71	0.48	5	5
7	0.00	0.00	0.00	0.00	0.00	0.00	5	5
8	0.00	0.00	0.00	0.00	0.00	0.00	5	5
9	0.50	1.00	1.00	0.80	0.91	0.89	5	5
10	1.00	0.00	1.00	0.00	1.00	0.00	5	5
11	0.83	1.00	1.00	0.80	0.91	0.89	5	5
12	0.62	0.00	1.00	0.00	0.77	0.00	5	5
13	0.00	0.00	0.00	0.00	0.00	0.00	5	5
14	1.00	0.00	1.00	0.00	1.00	0.00	5	5
15	0.71	0.00	1.00	0.00	0.83	0.00	5	5
16	1.00	0.50	1.00	1.00	1.00	0.67	5	5
17	0.00	0.00	0.00	0.00	0.00	0.00	5	5
18	1.00	0.00	1.00	0.00	1.00	0.00	5	5
19	1.00	0.00	1.00	0.00	1.00	0.00	5	5
20	1.00	0.25	1.00	1.00	1.00	0.40	5	5

Table B.1: Classification report for ERP data from Dataset 1 using 56 channels and 5 channels. Model trained on session 1 and validated on session 2.

Class	Precision		Recall		f1-score		support	
	Ch. 56	**Ch. 5**	**Ch. 56**	**Ch. 5**	**Ch. 56**	**Ch. 5**	**Ch. 56**	**Ch. 5**
1	1.00	0.67	1.00	0.40	1.00	0.50	5	5
2	1.00	0.28	1.00	1.00	1.00	0.43	5	5
3	1.00	0.36	1.00	1.00	1.00	0.53	5	5
4	0.00	1.00	0.00	1.00	0.00	1.00	5	5
5	1.00	1.00	1.00	1.00	1.00	1.00	5	5
6	1.00	1.00	1.00	0.20	1.00	0.33	5	5
7	1.00	0.00	1.00	0.00	1.00	0.00	5	5
8	0.00	0.00	0.00	0.00	0.00	0.00	5	5
9	0.50	0.50	1.00	1.00	0.67	0.67	5	5
10	0.00	0.00	0.00	0.00	0.00	0.00	5	5
11	1.00	0.00	1.00	0.00	1.00	0.00	5	5
12	1.00	1.00	1.00	1.00	1.00	1.00	5	5
13	1.00	0.00	1.00	0.00	1.00	0.00	5	5
14	1.00	0.00	1.00	0.00	1.00	0.00	5	5
15	0.50	0.56	1.00	1.00	0.67	0.71	5	5
16	0.50	0.50	1.00	1.00	0.67	0.67	5	5
17	0.50	0.00	0.00	0.00	0.00	0.00	5	5
18	1.00	1.00	1.00	1.00	1.00	1.00	5	5
19	0.00	0.00	1.00	0.00	0.00	0.00	5	5
20	0.50	1.00	1.00	1.00	0.67	1.00	5	5

Table B.2: Classification report for resting-state data from Dataset 1 using 56 channels and 5 channels. Model trained on session 1 and validated on session 2.

Class	Precision		Recall		f1-score		support	
	Ch. 56	**Ch. 5**	**Ch. 56**	**Ch. 5**	**Ch. 56**	**Ch. 5**	**Ch. 56**	**Ch. 5**
1	1.00	1.00	1.00	1.00	1.00	1.00	5	5
2	1.00	1.00	1.00	1.00	1.00	1.00	5	5
3	1.00	0.50	1.00	1.00	1.00	0.67	5	5
4	1.00	1.00	1.00	1.00	1.00	1.00	5	5
5	1.00	1.00	1.00	1.00	1.00	1.00	5	5
6	1.00	0.50	1.00	1.00	1.00	0.67	5	5
7	1.00	0.00	1.00	0.00	1.00	0.00	5	5
8	1.00	0.00	1.00	0.00	1.00	0.00	5	5
9	1.00	1.00	1.00	1.00	1.00	1.00	5	5
10	1.00	1.00	1.00	1.00	1.00	1.00	5	5
11	1.00	1.00	1.00	1.00	1.00	1.00	5	5
12	1.00	1.00	1.00	1.00	1.00	1.00	5	5
13	1.00	0.50	1.00	1.00	1.00	0.67	5	5
14	1.00	0.00	1.00	0.00	1.00	0.00	5	5
15	0.50	0.50	1.00	1.00	0.67	0.00	5	5
16	1.00	1.00	1.00	1.00	1.00	1.00	5	5
17	0.00	0.00	0.00	0.00	0.00	0.67	5	5
18	1.00	0.50	1.00	1.00	1.00	0.67	5	5
19	1.00	0.00	1.00	0.00	1.00	0.00	5	5
20	1.00	1.00	1.00	1.00	1.00	1.00	5	5

Table B.3: Classification report for resting-state data from Dataset 2 using 56 channels and 5 channels. Model trained on session 1 and validated on session 2.

Appendix C

API endpoints

The endpoints used in this work are part of a more extensive EEG-based biometric system. In fig. C.1, all the endpoints used in the biometric system are presented, including the HTTP method, data parameters used in the requests, and a short description of each endpoint.

Path	Method	Data parameters	Description
eeg/subject/add	POST	{ "application_id": 1, "name": subject1" }	Used to add a user to the system
eeg/data/save	POST	{ "application_id": 1, "feature_type": "dwt", "data": { "data": [[[-892.975, -869.8499, ... -888.98]]], "target": ["12", ... "12"] } }	Save EEG data in the database.
eeg/authentication/training	POST	{ "application_id": 1, "subject_id": 12, "model_type": single_model, “classifier”: “ocsvm”, "feature_type": "dwt" }	Train the authentication model
eeg/authentication/authorize	POST	{ "predicted_id": 12, "model_type": single_model, "feature_type": "dwt", "data": [[[-892.5, -869.849, ... ,-888.960128]] }	Check if subject is enrolled in the system
eeg/identification/training	POST	{ "application_id": 1, "feature_type": "dwt", "classifier": "svm” }	Create ML model for identification layer
eeg/identification/identify	POST	{ "feature_type": "dwt", "instance": [[[-892.905, -869.89, ... ,-888.960]]] }	Predict an identity for a subject

Figure C.1: Endpoints used in EEG-based Biometric System containing identification and authentication layer.

Shobiha K. Premkumar

Subject Identification using EEG Signals and Supervised Learning

NTNU
Norwegian University of
Science and Technology